Individualized Model Predictive Control for the Artificial Pancreas

IN SILICO EVALUATION OF CLOSED-LOOP GLUCOSE CONTROL

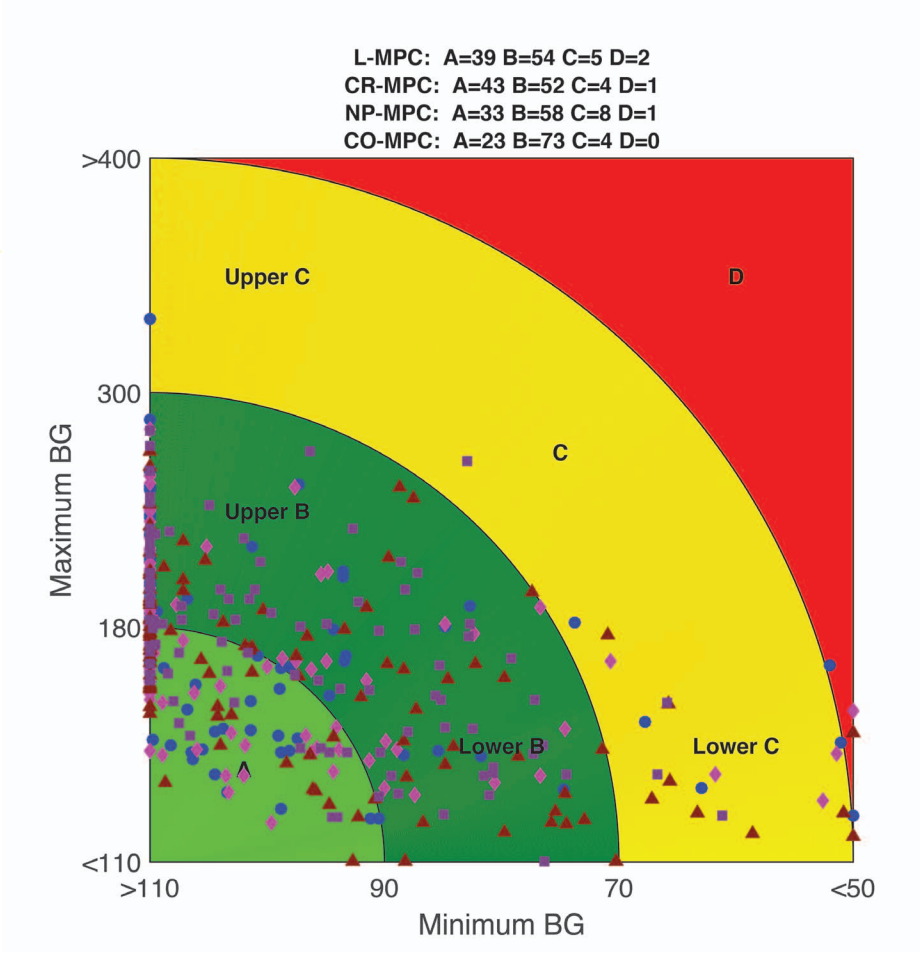

MIRKO MESSORI, GIAN PAOLO INCREMONA, CLAUDIO COBELLI, and LALO MAGNI

Digital Object Identifier 10.1109/MCS.2017.2766314
Date of publication: 19 January 2018

In each day of their lives, patients affected by type 1 diabetes (T1D) must maintain the blood glucose concentration (glycemia) within a safe range. T1D is a metabolic disorder characterized by a total insulin deficiency and, if not properly managed, would result in chronic hyperglycemia, thus increasing the risk of severe long-term complications. Insulin is a hormone

1066-033X/18©2018IEEE

allowing for the utilization of glucose by body tissue and suppression of liver glucose production. An insulin shortage must be compensated with exogenous administration. The external insulin supply avoids hyperglycemia but can cause hypoglycemia if the amount of needed insulin is overestimated. Hypoglycemia is associated with short-term complications, which in severe cases can result in coma or death. To properly estimate the needed quantity of insulin, T1D patients normally rely on conventional therapy, which is designed and continually updated by the physician, and consists of basal insulin (needed during fasting periods) and insulin boluses (needed to compensate for the glucose rise due to meals).

Insulin can be delivered by injections or infusions. The latter is less invasive and requires a subcutaneous insulin pump, which continuously releases microboluses in the interstitial tissues of the patient and can be programmed with a patient-specific conventional therapy. Subcutaneous glucose sensing is also possible by continuous glucose monitor (CGM) devices, which are able to read the interstitial glucose concentration and inform the patient about glycemia levels and trends. The availability of subcutaneous insulin pumps and CGM has allowed the realization of the sensor augmented pump (SAP) therapy, which assists the patient in maintaining the glucose concentration within a safe range. However, with an SAP, the patient still needs to decide how much insulin has to be infused by the pump on the basis of the CGM readings. The automation of the insulin infusion management can be reached with the artificial pancreas (AP), a system aimed at closed-loop glucose control.

The design of an AP dates from the 1970s, when the first experiments were conducted with highly invasive intravenous systems [1]. In the following years, AP systems have become progressively less invasive and more portable and, thanks to recent technological developments, newer AP systems have become wearable and usable in free-living conditions. Since the subcutaneous route for a fully automatic blood glucose control was shown to be feasible [1], [2], the AP architecture includes a subcutaneous insulin pump for insulin delivery (actuator), a CGM for glucose sensing (sensor), and a standalone device aimed at the execution of the control algorithm (controller) [3]. This architecture, which relies on wireless connections among all of the components, is the result of several clinical studies that were supported by the Juvenile Diabetes Research Foundation, the European Commission, and the National Institutes of Health [4]–[15].

The core of the AP is the control algorithm, which estimates the proper quantity of insulin to infuse in the subcutaneous tissues during fasting, meal, and postprandial periods. Beginning in 2008, several clinical trials were performed by relying on a model predictive control (MPC) algorithm [16]–[20] in a hospital setting [21]–[26]. Subsequently, an improved MPC algorithm [27] based on the achieved clinical results has been adapted for outpatient studies [28]. The aim was to move the AP to free-living conditions for long periods and, in 2014, an AP system equipped with the MPC algorithm [27] was used in the first randomized crossover outpatient clinical trial [15]. The AP was used for eight weeks during evening and night periods, paving the way for an extension study, completed in 2015, where the AP was continually used 24 h per day for one month [29]. The results showed that MPC, discussed in "Preliminaries on Model Predictive Control," is a promising and feasible approach for AP. However, since different patients are characterized by different glucose-insulin dynamics, the control algorithm must be designed with robustness properties to make the closed-loop glucose control reliable and safe for each patient without compromising the desirable performance. Different dynamics are caused by the intersubject variability, which reflects the different biological characteristics of each patient. Since an MPC algorithm determines the control actions on the basis of a model included in the cost function, patient-individualized glucose-insulin models are expected to further improve the glucose control performance. So far, the MPC used in the most recent clinical trials was synthesized on the basis of an average linear model [27]. The choice of using a linear model to describe the complex nonlinear glucose-insulin dynamics of diabetic patients is driven by the feasibility of the MPC implementation on a portable AP system [3], which is characterized by limited battery life and computational power. A similar approach (in which a compact model approximating the dynamics of the process under control was exploited to design the control law) was adopted in [30] in the context of type 2 diabetes. As discussed in "Summary," this article considers three techniques to synthesize customized MPC based on patient-tailored linear models. The final aim is to show through closed-loop simulations that customized MPC based on linear glucose-insulin models is able to improve the glucose control performance without losing the implementation feasibility on a portable AP device.

Preliminaries on Model Predictive Control

In several application contexts, there is the need to perform particularly critical tasks while fulfilling some plant constraints. MPC is one of the most effective solutions to this problem, as it can comply with large-scale systems with many control variables and provides a systematic method of dealing with constraints on inputs and states. MPC constraints are explicitly taken into account by solving an online CO problem used to determine the optimal inputs with respect to a predefined cost function. Typically, the optimization problem and the control law are defined in the discrete time domain, and the major requirements for its implementation are the model of the plant and a cost function to optimize.

Consider the discrete-time linear system

$$x(k+1) = Ax(k) + Bu(k) + Md(k), \tag{S1}$$

where $x(k) \in \mathbb{R}^n$ is the state vector, $u(k) \in \mathbb{R}^m$ is the input vector, and $d(k) \in \mathbb{R}^l$ is a disturbance vector at the kth sampling time instant. Also, $A \in \mathbb{R}^{n\times n}, B \in \mathbb{R}^{n\times m}$, and $M \in \mathbb{R}^{n\times l}$ are the system matrices, and N denotes the prediction horizon. Given a predicted input sequence

$$U(k) = [u^T(k \mid k), u^T(k+1 \mid k), \ldots, u^T(k+N-1 \mid k)]^T$$

and a disturbance sequence

$$D(k) = [d^T(k), d^T(k+1), \ldots, d^T(k+N-1)]^T,$$

the time evolution of the state is generated by simulating the model (S1) forward for N sampling time intervals with initial condition $x(k \mid k) = x(k)$. Consequently,

$$X(k+1) = [x^T(k+1 \mid k), x^T(k+2 \mid k), \ldots, x^T(k+N \mid k)]^T,$$

with $u(k+i \mid k)$ and $x(k+i \mid k), i \in \mathbb{N}$, being the input and state at time $k+i$ predicted at time k. The control input applied to the plant is generated by solving an optimization problem driven by a prespecified cost function to be minimized, for instance,

$$J(x(k), U(\cdot), k) = \sum_{i=0}^{N-1} \left\| x(k+i \mid k) - x_{\text{ref}}(k+i) \right\|_Q^2 + \left\| u(k+i \mid k) - u_{\text{ref}}(k+i) \right\|_R^2, \tag{S2}$$

with $x_{\text{ref}}(k)$ and $u_{\text{ref}}(k)$ denoting the states and inputs references at time k, respectively, included in the reference vectors

$$\begin{aligned} U_{\text{ref}}(k) &= [u_{\text{ref}}^T(k), u_{\text{ref}}^T(k+1), \ldots, u_{\text{ref}}^T(k+N-1)]^T, \\ X_{\text{ref}}(k) &= [x_{\text{ref}}^T(k), x_{\text{ref}}^T(k+1), \ldots, x_{\text{ref}}^T(k+N-1)]^T, \end{aligned} \tag{S3}$$

and where Q and R are symmetric positive definite matrices. The goal is to find the optimal control sequence $U^o(k)$ such that

$$U^o(k) = \arg\min_U J(x(k), U(\cdot), k),$$

subject to the model (S1) and possibly including input and state constraints.

Finally, after the generation of the control input and according to the receding horizon approach, only the first element of the optimal control sequence $U^o(k)$ is applied to the plant $u(k) = u^o(k \mid k)$. The optimization process is then repeated at each sampling time k.

The in silico results are presented, and, to quantify the benefits of the customized MPC, a statistical comparison on the outcome metrics is performed versus the noncustomized MPC.

GLUCOSE-INSULIN MODELS

The availability of a model describing the patient glucose-insulin dynamics is mandatory to synthesize an effective MPC. One of the main components of an MPC algorithm is a model describing the dynamics of the process under control (see "Preliminaries on Model Predictive Control"). In the context of AP, the reliability of the model glucose predictions are directly correlated to the efficacy of the controller, which commands the pump with the proper insulin to be infused as microboluses. A model able to predict the patient glycemia would be able to adjust the controller behavior to maintain the blood glucose concentration within the euglycemic range, which spans from 70 to 180 mg/dl, thus minimizing the risk of possible hyper- and hypoglycemia. However, methods used to directly measure the individual parameters of a T1D patient are invasive and expensive, making the identification of individualized glucose-insulin models a challenging task.

UVA/Padova Simulator

Several research groups have developed glucose-insulin models [31]–[33]. Of particular interest is the model developed by the Universities of Virginia and Padova (UVA/Padova) [34], which was included in the first simulator accepted by the U.S. Food and Drug Administration as a substitute to animal trials for preclinical testing of insulin therapies for T1D patients. The model included in the simulator is able to simulate the glucose-insulin dynamics of a specific person and belongs to the class of compartmental models, of which a brief introduction is presented in "Compartmental Models." The structure of the UVA/Padova simulator model is depicted in Figure 1. Different dynamics for different people are simulated due to the availability of various sets of key metabolic parameters that describe the intersubject variability of a generic population of T1D patients. Each set of parameters represents a "virtual subject" and has been identified from

As previously discussed, one of the features of MPC is the presence of input and state constraints in the optimization problem. In addition to the equality constraints representing the model dynamics (S1), inequality constraints on input and state variables can be introduced. While the equality constraints are usually handled implicitly to compute predicted state trajectories as functions of initial conditions and input trajectories, the inequality constraints are explicitly imposed within the optimization problem.

The cost function defined in (S2) can be enriched with a weight associated with the state prediction at the horizon N. This modification can be performed by considering the quadratic cost function

$$J(x(k),U(\cdot),k)=\sum_{i=0}^{N-1}\|x(k+i\,|\,k)-x_{\text{ref}}(k+i)\|_Q^2 + \|u(k+i\,|\,k)-u_{\text{ref}}(k+i)\|_R^2+\|x(k+N\,|\,k)\|_P^2, \tag{S4}$$

subject to the state dynamics (S1), with P being the unique nonnegative solution of the discrete time Riccati equation

$$P(k)=Q+A^TP(k+1)A-A^TP(k+1)B \times(R+B^TP(k+1)B)^{-1}B^TP(k+1)A. \tag{S5}$$

The matrix $P\in\mathbb{R}^{n\times n}$ is the weight related to the term $x(k+N\,|\,k)$, which represents the predicted state at the horizon N. P takes into account the cost over an infinite horizon. By considering the horizon N, the predicted state trajectories of the system dynamics can be written as

$$X(k+1)=\mathcal{A}x(k)+\mathcal{B}U(k)+\mathcal{M}D(k),$$

where the matrices $\mathcal{A}\in\mathbb{R}^{nN\times n}$, $\mathcal{B}\in\mathbb{R}^{nN\times mN}$, and $\mathcal{M}\in\mathbb{R}^{nN\times lN}$ are obtained through algebraic calculations based on (S1). In the general case, $D(k)$ can be known, estimated, or unknown depending on the specific application to control. In the case of unknown disturbance, the MPC calibration achieved through the Q and R parameters of (S4) must be robust enough to guarantee at least suboptimal (but safe) control performance. Thus, the cost (S4) can be rewritten as

$$J(x(k),U(\cdot),k)=\|U(k)\|_{\mathcal{H}}^2+2(x^T(k)\mathcal{F}_x^T+D^T(k)\mathcal{F}_D^T - U_{\text{ref}}^T(k)\mathcal{R}-X_{\text{ref}}^T(k)\mathcal{F}_{X_{\text{ref}}}^T)U(k),$$

where only the terms depending on $U(k)$ have been maintained and $\mathcal{H}=\mathcal{B}^T\mathcal{Q}\mathcal{B}+\mathcal{R}$, $\mathcal{F}_x=\mathcal{B}^T\mathcal{Q}\mathcal{A}$, $\mathcal{F}_D=\mathcal{B}^T\mathcal{Q}\mathcal{M}$, and $\mathcal{F}_{X_{ref}}=\mathcal{B}^T\mathcal{Q}$, with $\mathcal{Q}=\text{diag}(Q,\ldots,Q)\in\mathbb{R}^{nN\times nN}$ and $\mathcal{R}=\text{diag}(R,\ldots,R)\in\mathbb{R}^{mN\times mN}$.

If the optimization problem does not take into account input and state constraints, under the assumption of nonsingularity of the matrix $\mathcal{H}$, the solution exists, is unique, and can be explicitly written as

$$U^o(k)=\mathcal{H}^{-1}(-\mathcal{F}_x x(k)-\mathcal{F}_D D(k)+\mathcal{R}U_{ref}(k)+\mathcal{F}_{X_{ref}}X_{ref}(k)).$$

On the other hand, in the case of constraints on input or states, the optimization problem must be solved online through a quadratic programming optimizer.

a large nondiabetic subject database, where each subject underwent a triple tracer meal protocol that provided quasi-model-independent estimates of glucose and insulin fluxes [32]. The model was subsequently adapted to T1D by incorporating a model of subcutaneous insulin absorption and was shown to reliably describe the T1D literature data. Three "virtual populations" (children, adolescents, and adults), each comprised of 100 subjects, were included in the simulator [34]. The UVA/Padova model was then refined by improving the hypoglycemia glucose kinetics (by adding glucagon kinetics and secretion) and refining the virtual subjects included in the simulator [35] (see Figure 2). The clinical validity of the model was assessed on T1D data [36], and the circadian variability of insulin sensitivity (IS) and meal absorption parameters were also included in the most recent version of the simulator [37], [38].

Nonlinear Time-Variant Model

The complete state-space representation of the nonlinear, time-variant, compartmental model depicted in Figure 1 is

$$\begin{cases}
\dot{x}_1(t)=-k_{gri}x_1(t)+d(t),\\
\dot{x}_2(t)=k_{gri}x_1(t)-k_{empt}(x_1(t)+x_2(t))x_2(t),\\
\dot{x}_3(t)=-k_{abs}x_3(t)+k_{empt}(x_1(t)+x_2(t))x_2(t),\\
\dot{x}_4(t)=EGP(t)+Ra(t)-U_{ii}(t)-E(t)-k_1x_4(t)+k_2x_5(t),\\
\dot{x}_5(t)=-U_{id}(t)+k_1x_4(t)-k_2x_5(t),\\
\dot{x}_6(t)=-(m_2+m_4)x_6(t)+m_1x_{10}(t)+k_{a1}x_{11}(t)+k_{a2}x_{12}(t),\\
\dot{x}_7(t)=-p_{2U}x_7(t)+p_{2U}\left(\dfrac{x_6(t)}{V_I}-I_b\right),\\
\dot{x}_8(t)=-k_ix_8(t)+k_i\dfrac{x_6(t)}{V_I},\\
\dot{x}_9(t)=-k_ix_9(t)+k_ix_8(t),\\
\dot{x}_{10}(t)=-(m_1+m_3(t))x_{10}(t)+m_2x_6(t),\\
\dot{x}_{11}(t)=-(k_d+k_{a1})x_{11}(t)+i(t),\\
\dot{x}_{12}(t)=k_dx_{11}(t)-k_{a2}x_{12}(t),\\
\dot{x}_{13}(t)=-k_{sc}x_{13}(t)+k_{sc}x_4(t),\\
\dot{x}_{14}(t)=-n_Gx_{14}(t)+SR_H(t),\\
\dot{x}_{15}(t)=-k_Hx_{15}(t)+k_H\max\{x_{14}(t)-H_b,0\},\\
\dot{x}_{16}(t)=\dot{S}R_H^s(t),
\end{cases} \tag{1}$$

where the definitions of all the states $x_i(t), i=1,\ldots,16$ are shown in Table 1. This model is included in the UVA/Padova simulator and characterized by the set of parameters listed

Summary

T1D is a metabolic disorder that causes a total insulin deficiency and impedes the regulation of blood glucose concentration (also called glycemia) by the pancreas. Insulin is an essential hormone for blood glucose control, and the lack of insulin could result in chronic hyperglycemia, which exposes T1D subjects to risky long-term complications. The lack of insulin must be compensated with exogenous, usually subcutaneous, insulin administration that can result in hypoglycemia if the amount of insulin is overestimated. Hypoglycemia is associated with short-term complications that, in severe cases, can result in a coma or death. Consequently, T1D subjects face the challenge of maintaining their glycemia within a safe range. An AP is a system devoted to the automatic regulation of exogenous insulin administration. Initial AP realizations used the intravenous route for insulin administration and were thus highly invasive. Current AP systems rely on subcutaneous insulin pumps for insulin infusions and subcutaneous glucose sensors for glycemia measurements. The loop is closed through a control algorithm implemented on a portable device that evaluates the needed quantity of insulin based on the subjects' state, which is estimated using the subcutaneous glucose sensing. The subcutaneous route for glucose sensing and insulin infusion is well suited for 24-h use of the AP system. However, this architecture is affected by inherent delays in both sensing and (especially) actuation, which motivate the need for advanced control techniques. MPC has been used extensively as an AP control algorithm in several clinical trials completed in hospital, outpatient, and, more recently, free-living conditions. The results show that it is a feasible approach for the AP. However, because T1D subjects have different glucose-insulin dynamics, the control algorithm must be robust to ensure that the closed-loop glucose control is reliable and safe for each subject without significantly compromising the performance. Different dynamics reflect the different biological characteristics of each subject, and, since the MPC algorithm determines the control actions through a model included in the cost function, subject-individualized models are expected to improve the AP performance. This article considers three individualization techniques to synthesize customized MPC based on tailored linear models. The individualized glucose-insulin models are presented first and subsequently included in an exhaustive description of the MPC algorithm used in the AP system. For each of the individualized techniques, results of closed-loop simulations performed on the adult virtual population of the UVA/Padova simulator are presented. These results are then compared with the results achieved through an MPC driven by the average model adopted in several clinical trials. The final aim is to show that customized MPCs are able to improve the glucose control performance without losing safety and implementation feasibility on a portable AP device, thus taking a significant step towards making individualized AP systems usable in vivo.

in Table 2. Each set of parameter defines a virtual subject, and a set of virtual subjects defines a virtual population (Figure 2). The considered inputs are $i(t)$ and $d(t)$, which represent the exogenous subcutaneous insulin infusion and the meal intake, respectively. The measurable output is the subcutaneous glucose concentration, which is calculated by dividing the glucose contained in the subcutaneous glucose compartment x_{13} by the compartment volume V_G. More details on this model, the numerical values of the constant parameters, and the definition of the time-varying parameters are available in [34] and [35].

Linearized Average Model

The UVA/Padova model is highly nonlinear and time variant, and its incorporation in an MPC algorithm is computationally demanding, making the implementation on a portable AP device [3] practically unfeasible. Moreover, the key metabolic parameters associated with the nonlinear glucose-insulin dynamics of an individual are unknown, thus preventing the direct use of the UVA/Padova model for synthesizing an MPC suitable for clinical purposes.

Since the virtual population is thought to statistically represent the intersubject variability of a generic population of T1D patients, an average time-invariant model representing the average dynamics of a diabetic patient can be computed by substituting all the time-varying parameters with their average values and then by averaging all the available sets of key metabolic parameters (see Table 2). The average parameters are imposed in the model (1), which is subsequently linearized around a fictitious basal equilibrium corresponding to the basal glucose G_b, a steady-state condition reached during fasting periods by infusing only basal insulin i_b [20]. Thus, by imposing $i(t) = i_b(t)$ and $d(t) = 0$, the model reaches the fasting steady-state equilibrium and is subsequently linearized to obtain a linear model defined as

$$\begin{cases} x(k+1) = Ax(k) + Bu(k) + Md(k), \\ y(k) = Cx(k), \end{cases} \tag{2}$$

where $u(k)$ (pmol/t_s) and $d(k)$ (mg/t_s) are the variation of the subcutaneous insulin infusion with respect to the basal insulin and the meal intake, respectively; and $y(k)$ (mg/dl) is the variation of the subcutaneous glucose concentration with respect to the fasting basal glucose G_b. Model (2) is written in state-space form and is characterized by the state

Compartmental Models

Compartmental models are represented by a set of compartments that can send control signals to other compartments and contain material that can be exchanged with other compartments. The generic equation that describes the quantity of material contained in a specific compartment is

$$\dot{Q}_m^i(t) = \sum_{\substack{j=1 \\ j\neq i}}^{N_c} R_{ij} - \sum_{\substack{j=1 \\ j\neq i}}^{N_c} R_{ji}, \qquad i = 1, \ldots, N_c, \tag{S6}$$

where Q_m^i is the quantity of material of the ith compartment, N_c is the total number of compartments, R_{ij} is the incoming flux of material from compartment j to compartment i, and R_{ji} is the outgoing flux from compartment i to compartment j. A set of equations of the form of (S6) describes the relationships among compartments, defining the whole system dynamics. The flow rate between two compartments can be described by linear or nonlinear laws. Examples of nonlinear laws are [S1]

$$\begin{aligned} R_{ij}(Q_m^j(t)) &= \frac{V_{\max} \cdot Q_m^j(t)^{k_1 - 1}}{K_m + Q_m^j(t)^{k_1}}, \\ R_{ij}(Q_m^j(t)) &= \frac{V_{\max}}{K_m + Q_m^j(t)}, \\ R_{ij}(Q_m^j(t)) &= \begin{cases} k_2\left(1 - \dfrac{Q_m^i(t)}{k_3}\right) & Q_m^i(t) < k_3, \\ 0 & Q_m^i(t) \geq k_3, \end{cases} \end{aligned} \tag{S7}$$

where k_1, k_2, and k_3 are constants and K_m and $V_{\max}$ are rate parameters. The flux can be also described by a linear relationship

$$R_{ij}(Q_m^j(t)) = k_{ij} Q_m^j(t), \tag{S8}$$

where k_{ij} is the rate constant associated with the incoming flux from compartment j to compartment i. When a compartmental model is used to represent a biological system, each compartment usually represents a part of the body that contains a specific material. For instance, in a very simplified human body representation, the stomach and the blood compartments can be defined, as shown in Figure S1. If the material is an oral drug, the first represents the drug concentration into the stomach, and the second represents the drug concentration into the blood. The two compartments together represent a simplified whole-body model of the drug, starting from the oral intake [$u(t)$, the system input], the absorption in the bloodstream [driven by the flux $R_{21}(Q_m^1(t))$], and the excretion [driven by the excretion rate $R_{02}(Q_m^2(t))$]. The fluxes describing the way the drug is absorbed in/or excreted from the blood compartment can be represented by any nonlinear or linear relationship, like (S7) or (S8). In the graphical representation of compartmental models, the accessible compartments from outside are denoted with a dashed line with a bullet. The blood compartment of Figure S1 is denoted as accessible because of the possibility to measure the drug concentration in the blood of the patient. Moreover, if compartment i is controlled from compartment j, this action is represented by a dashed arrow.

State-Space Representation

Compartmental models can be described with a state-space representation where the quantities of material in each compartment represent the model states. The state-space representation of the model depicted in Figure S1 is

$$\begin{cases} \dot{x}_1(t) = -R_{21}(x_1(t)) + u(t), \\ \dot{x}_2(t) = R_{21}(x_1(t)) - R_{02}(x_2(t)), \\ y(t) = \dfrac{x_2(t)}{V_2}, \end{cases}$$

where $x_1(t) = Q_m^1(t), x_2(t) = Q_m^2(t)$, $u(t)$ is the system input (oral drug intake), $y(t)$ is the system output (drug concentration measured in the blood), and V_2 is the volume of the blood compartment.

REFERENCE

[S1] C. Cobelli and E. Carson, *Introduction to Modeling in Physiology and Medicine*. New York: Academic, 2008.

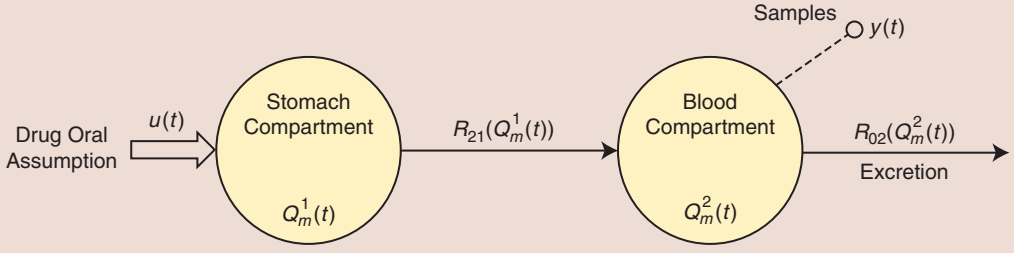

FIGURE S1 An example of a compartmental model with two compartments. The first is the stomach compartment, and the second is the blood compartment. The open arrow represents the drug oral intake $u(t)$ (system input), the black arrows represent the flow rates, and the dashed line represents the samples $y(t)$ taken from the blood compartment (system output). The drug quantity in the stomach $Q_m^1(t)$ is transferred in the blood compartment through the flow rate $R_{21}(Q_m^1(t))$. The drug quantity in the blood compartment $Q_m^2(t)$ is finally excreted through the excretion rate $R_{02}(Q_m^2(t))$.

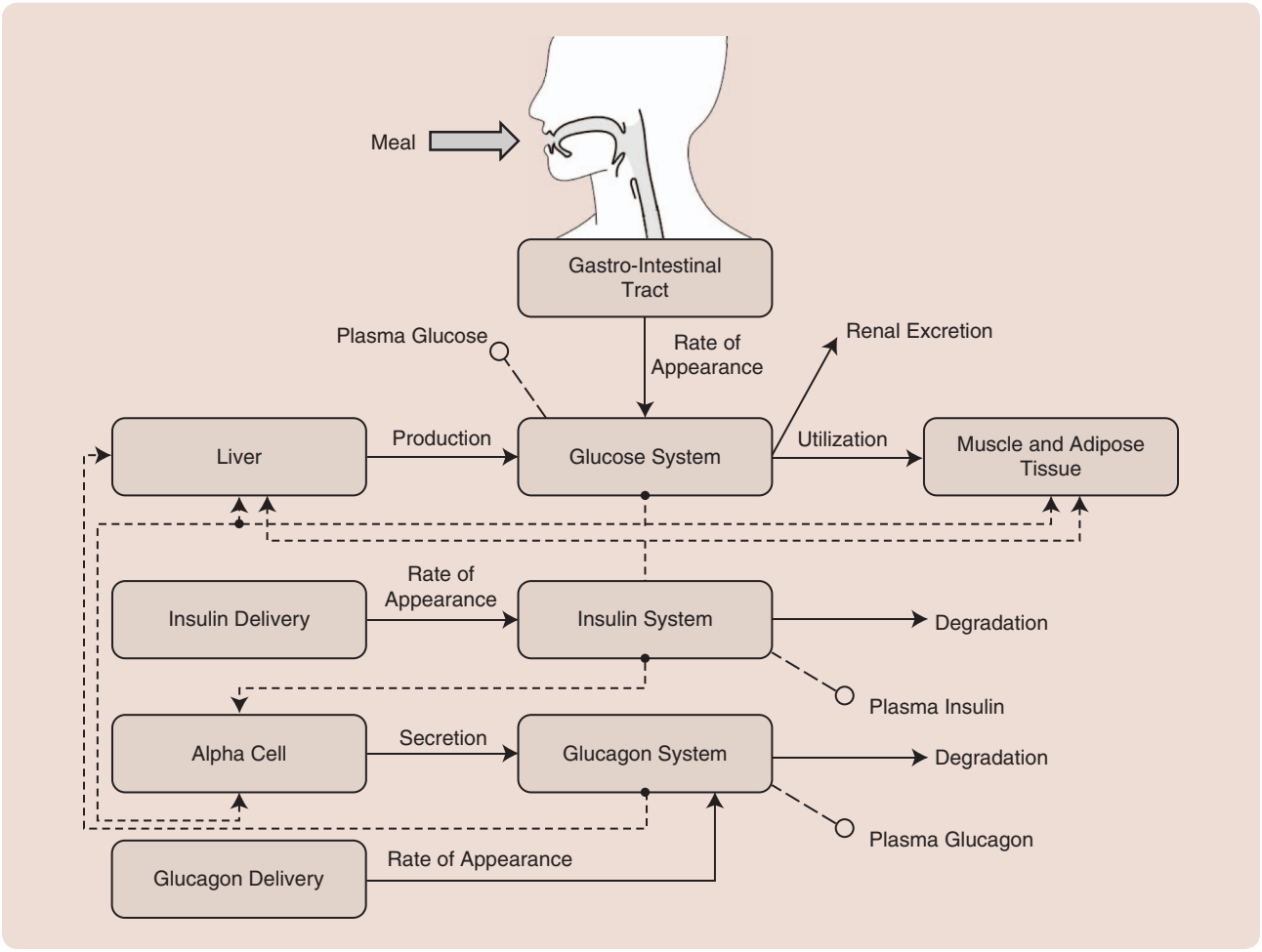

FIGURE 1 A compartmental representation of the glucose-insulin model included in the UVA/Padova simulator [35]. The fluxes of material are represented by the solid arrows, the dashed arrows represent control signals between compartments, and the dashed lines linked to empty circles represent the accessible compartments.

matrix A, a square matrix containing information about the relationships among all states. Several simulations have shown that the states $x_{14}(t)$, $x_{15}(t)$, and $x_{16}(t)$ of (1), which are associated with the glucagon system of Figure 1, can be neglected in the linear model without affecting the MPC performance. Thus, $A \in \mathbb{R}^{n\times n}$, with $n = 13$ denoting the total number of states of the linear model. Since the MPC algorithm running on the controller device is characterized by a sampling time t_s, model (2) is represented in discrete-time form. The average linearized model (2) synthesizes a nonindividualized MPC with average glucose-insulin dynamics. This control approach, of which a detailed description can be found in [20] and [27], has been utilized in several clinical trials performed in both adults [13], [15], [26], [28] and children [39].

Customized Linear Models

A nonindividualized MPC based on an average model can be substantially penalized by the intersubject variability affecting T1D patients. The latter can be handled by model customization, thus defining models that synthesize MPC to improve the glucose control performance. In this section, three model customization techniques are presented, in which two identify individualized models that reproduce patient-specific glucose-insulin dynamics. All customized models are characterized by the same inputs and output of the linearized average model (2).

CR-Based Models

The model customization approach described in [40] is based on subdividing the entire virtual population in subgroups. Each group is defined by considering the insulin-to-carbohydrate ratio (CR) parameter of each virtual subject. CR is a parameter that is part of the conventional therapy of the patient and represents the nominal quantity of insulin bolus needed to compensate a meal through the relationship

$$i_B^{CR}(k) = \frac{d^g(k)}{CR(k)}, \tag{3}$$

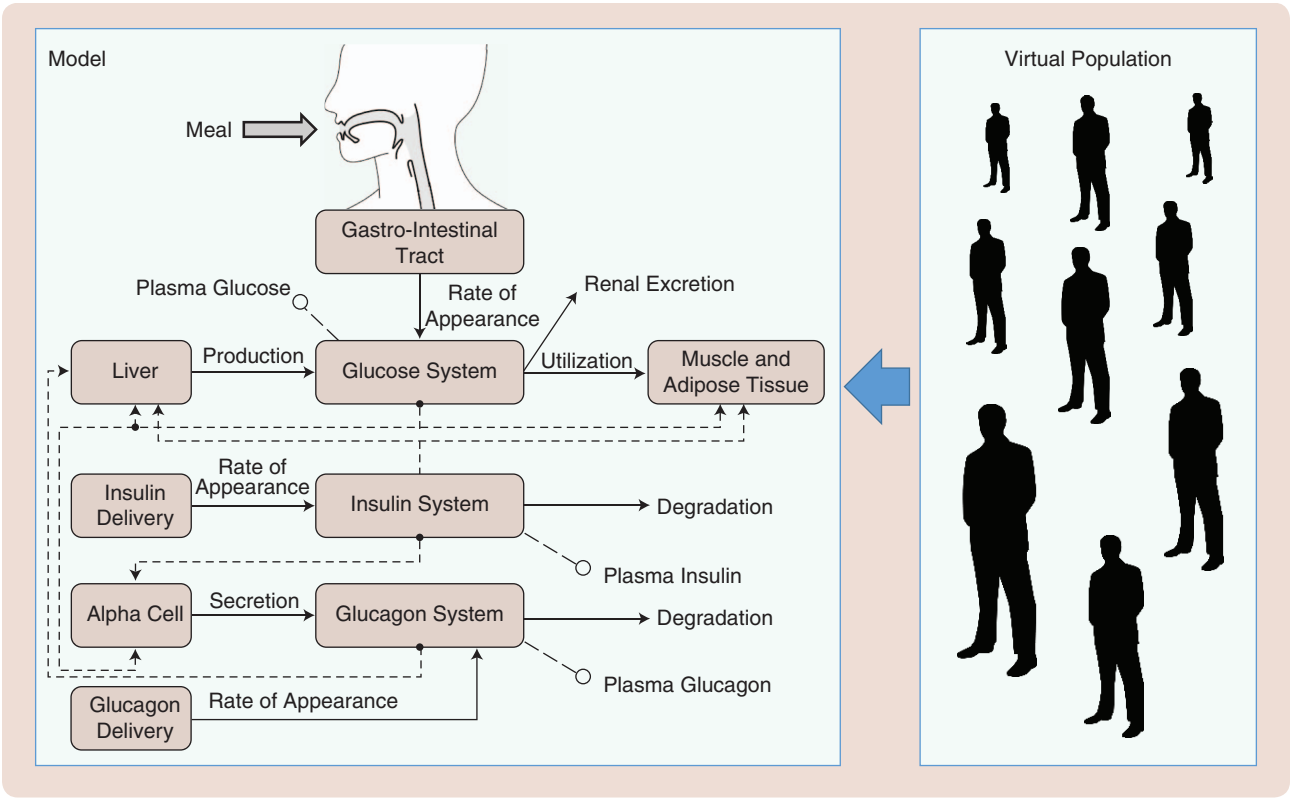

FIGURE 2 A virtual population is composed of several "virtual subjects." Each virtual subject is characterized by a set of key metabolic parameters of the glucose-insulin model. A virtual population is thought to span the intersubject variability that can be encountered in a population of patients affected by type 1 diabetes.

where $i_B^{CR}(k)$ (U) is the nominal insulin bolus that must be infused to compensate for the estimated quantity of carbohydrates (CHO) included in the meal $d^g(k)$ (g), and $CR(k)$ (g/U) is the CR value at time k, retrieved by considering the daily patient CR pattern. The subdivision presented in [40] defines four subgroups of the adult virtual population of the UVA/Padova simulator, each of which is composed of patients having low, medium-low, medium-high, and high IS. The subgroups are defined as

$$\begin{cases} \text{1st Group:} & \overline{CR} \le 12 & \text{28 patients, low IS,} \\ \text{2nd Group:} & 12 < \overline{CR} \le 15 & \text{21 patients, medium-low IS,} \\ \text{3rd Group:} & 15 < \overline{CR} \le 19 & \text{21 patients, medium-high IS,} \\ \text{4th Group:} & \overline{CR} > 19 & \text{30 patients, high IS,} \end{cases} \tag{4}$$

with $\overline{CR}$ representing the average value of the daily CR pattern and where 12, 15, and 19 are the integer approximations of the 25th, 50th, and 75th percentiles associated with the CR distribution of the adult virtual population (see Figure 3). For each subgroup, an average model is computed and then linearized around the basal equilibrium, thus obtaining four linear models in the form of (2), which can be used to synthesize an MPC. The customization consists of synthesizing the MPC by selecting the most appropriate model for a generic patient by considering his/her $\overline{CR}$ value. This value is used to determine the group to which the patient belongs.

Nonparametric Models

The CR-based customization approach defines a set of models that can be used to synthesize a customized MPC based on the patient's estimated IS. However, further improvements are expected in closed-loop glucose control with MPC based on patient-tailored models that incorporate patient-specific, glucose-insulin dynamics. The nonparametric (NP) approach described in [41] belongs to the class of black-box identification and can be used to identify patient-specific glucose-insulin models by relying on historical insulin administrations and meal intakes (inputs), and CGM measurements (output). Given a set of historical input–output data associated with a specific patient, the NP approach identifies a one-step ahead predictor that is subsequently converted in a state-space model obtained through a minimal realization of a given dimension. The identification process is performed through a kernel-based regression in which the stable spline kernel introduced in [42] is considered. The final result is the identification of a linear time-invariant model having the form

$$y(t) = \sum_{k=1}^{p_l} q_u(k)u(t-k) + \sum_{k=1}^{p_l} q_d(k)d(t-k) + \sum_{k=0}^{p_l} w(k)e(t-k), \tag{5}$$

TABLE 1 State variables associated with the state-space system (1).

State	Meaning	Unit
x_1	Stomach first compartment	mg
x_2	Stomach second compartment	mg
x_3	Intestine	mg
x_4	Plasma glucose and insulin-independent tissues	mg/kg
x_5	Insulin-dependent tissues	mg/kg
x_6	Plasma insulin	pmol/kg
x_7	Insulin action	pmol/l
x_8	Delay compartment for insulin action on glucose production	pmol/l
x_9	Insulin action on glucose production	pmol/l
x_{10}	Insulin in the liver	pmol/kg
x_{11}	First compartment of subcutaneous insulin	pmol/kg
x_{12}	Second compartment of subcutaneous insulin	pmol/kg
x_{13}	Subcutaneous glucose	mg/kg
x_{14}	Plasma glucagon	ng/dl
x_{15}	Glucagon action	ng/dl
x_{16}	Delayed static glucagon secretion	ng/dl/min

where $e(k)$ is a white Gaussian noise signal representing the uncertainties affecting the model and where the Z-transforms of $q_u(k)$, $q_d(k)$, and $w(k)$ are given by

$$Q_u(z)=\frac{\sum_{k=1}^{p_l} g_1(k)z^{-k}}{1-\sum_{k=1}^{p_l} f(k)z^{-k}},\quad Q_d(z)=\frac{\sum_{k=1}^{p_l} g_2(k)z^{-k}}{1-\sum_{k=1}^{p_l} f(k)z^{-k}},$$
$$W(z)=\frac{1}{1-\sum_{k=1}^{p_l} f(k)z^{-k}}, \tag{6}$$

with p_l denoting a tunable parameter. The quantities g_1, g_2, and f represent the impulse responses related to insulin, meals, and the Gaussian noise and are identified through the kernel-based regression process. Thus, the individualized MPC is synthesized by relying on the following state-space augmented model achieved through minimal realization:

$$\begin{cases} x_{\mathrm{NP}}(k+1)=A_{\mathrm{NP}}x_{\mathrm{NP}}(k)+B_{\mathrm{NP}}u(k)+M_{\mathrm{NP}}d(k)+W_{\mathrm{NP}_x}e(k),\\ y(k)=C_{\mathrm{NP}}x_{\mathrm{NP}}(k)+W_{\mathrm{NP}_y}e(k), \end{cases} \tag{7}$$

where x_{NP} is a vector of maximum dimension p_l containing the internal states; A_{NP}, B_{NP}, C_{NP}, and M_{NP} are matrices of proper dimensions; W_{NP_x} is a column vector (with maximum dimension p_l); and W_{NP_y} is a scalar value.

Constrained Optimization Models

As a black-box identification technique, the NP approach identifies linear models with an unknown internal structure. Indeed, there is no control on the achievable number of internal states, which can only be limited to p_l, a parameter that must be large enough to capture the essential dynamics of the patient. Having a linear model with a large number of internal states could be an issue for the MPC algorithm implementation, which must reside on a standalone device with limited computational power and memory. To identify a linear model having a fixed parametric structure, the gray-box identification approach based on the constrained optimization (CO) process described in [41] is considered. By considering the linearization of the UVA/Padova model (1) around the basal equilibrium point, the parametric model structure

$$\begin{cases} x_{\mathrm{CO}}(k+1)=A_{\mathrm{CO}}x_{\mathrm{CO}}(k)+B_{\mathrm{CO}}u(k)+M_{\mathrm{CO}}d(k),\\ y(k)=C_{\mathrm{CO}}x_{\mathrm{CO}}(k), \end{cases} \tag{8}$$

having the same form of (2) is postulated, where x_{CO} is a vector containing the $n=13$ model states, and the matrices $A_{\mathrm{CO}}\in\mathbb{R}^{n\times n}$, $B_{\mathrm{CO}}\in\mathbb{R}^{n\times 1}$, $C_{\mathrm{CO}}\in\mathbb{R}^{1\times n}$, and $M_{\mathrm{CO}}\in\mathbb{R}^{n\times 1}$ are identified through the solution of the CO problem described in [41]. The identification is performed by relying on historical input–output data associated with the patient.

In contrast to the NP approach, the CGM subcutaneous glucose measurements (output data) need to be prefiltered to be considered for identification. The prefiltering is used to reduce the noise component affecting the CGM measurements, which could significantly reduce the identifiability of the patient glucose-insulin dynamics. The prefiltering process can be performed with several techniques. A simple technique considers the moving average filter

$$y_{\mathrm{MA}}(k)=\frac{\sum_{j=0}^{N_{\mathrm{MA}}-1}\mathrm{CGM}(k-j)}{N_{\mathrm{MA}}},$$

where y_{MA} (mg/dl) is the prefiltered output data used in the identification process, $\mathrm{CGM}(k)$ is the measured subcutaneous glucose by the CGM at time k, and N_{MA} is the considered moving average length. Prefiltering techniques that are more specific for CGM measurements can also be considered, like the retrofitting process described in [43]. Despite the need for prefiltering, a substantial advantage of the CO approach with respect to the NP is represented by the fixed parametric structure of the identified model, which results in a fixed implementation complexity of the MPC algorithm for any patient. Moreover, it has been shown that the CO approach is able to capture the glucose-insulin dynamics of the patient by relying on shorter

TABLE 2 Inputs, output, and key metabolic parameters associated with the state-space system (1).

	Symbol	Meaning	Unit
Model inputs	$i(t)$	Exogenous insulin infusion rate	pmol/kg/min
	$d(t)$	Ingested meal	mg/min
Model output	$\frac{x_{13}(t)}{V_G}$	Subcutaneous glucose concentration	mg/dl
Constant parameters	$k_{gri},\ k_{abs}$	Rate parameters	min^{-1}
	$k_1,\ k_2,\ k_{a1}, k_{a2}$		
	$m_1,\ m_2,\ m_4,\ p_{2U}$		
	$k_i,\ k_d,\ k_{sc},\ k_H,\ n_G$		
	V_I	Distribution volume of insulin	l/kg
	V_G	Distribution volume of glucose	dl/kg
	I_b	Model basal insulin	pmol/l
	H_b	Model basal glucagon	ng/dl
Time-varying parameters	$k_{empt}(t)$	Gastric emptying coefficient	min^{-1}
	$Ra(t)$	Glucose rate of appearance	mg/kg/min
	$EGP(t)$	Endogenous glucose production	mg/kg/min
	$E(t)$	Renal excretion	mg/kg/min
	$U_{ii}(t)$	Insulin-independent utilization	mg/kg/min
	$U_{id}(t)$	Insulin-dependent utilization	mg/kg/min
	$m_3(t)$	Linear degradation coefficient	min^{-1}
	$SR_H(t)$	Glucagon secretion	ng/dl/min
	$SR_H^s(t)$	Delayed static glucagon secretion	ng/dl

identification data sets [41], which are more easily realizable in a real-life scenario where the patient would be enrolled in a clinical study to produce historical input–output data for identification purposes.

CLOSED-LOOP GLUCOSE CONTROL

The presented identification approaches identify individualized glucose-insulin models to be included in the MPC algorithm, thus defining an individualized control law for the AP system. Preliminary closed-loop results were obtained in silico through customized MPC with CR-based models [40] and individualized MPC based on NP [44] models. In this article, these closed-loop results are refined and compared with the results achieved in closed-loop through the individualized MPC based on the CO models.

A schematic AP representation is depicted in Figure 4. The MPC algorithm is the core of the AP and must properly command the insulin pump on the basis of CGM subcutaneous glucose readings. Of particular interest are the meals, which are considered substantial disturbances affecting the glucose concentration and handled through the meal announcement, a feedforward action controlled by the patient [20]. The MPC algorithm can also use information contained in the conventional therapy, which is adapted to the patient and continually updated by the physician.

Conventional Therapy

Diabetic patients can rely on the conventional therapy, which is adapted by the physician to the patient. Conventional therapy consists of the basal insulin (the insulin needed to maintain the patient glycemia at a target during fasting periods) and the insulin bolus (the insulin needed to compensate for the increase in glycemia due to a meal). The insulin suggested by the conventional therapy is defined as

$$i(k) = i_B(k) + i_b^U(k),$$

where $i_B(k)$ (U) is the insulin bolus associated with the meal consumed at time k, and $i_b^U(k)$ (U) is the patient basal insulin, usually represented as a piecewise constant function.

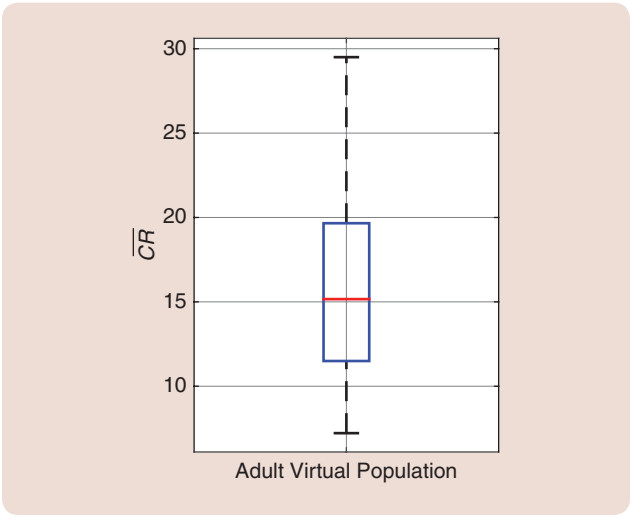

FIGURE 3 The distribution of the average daily insulin-to-carbo ratio patterns ($\overline{CR}$) associated with the adult virtual population of the UVA/Padova simulator. For each virtual subject, a pattern is known and used to build the box plot, which is composed of 100 values. As specified in (4), the integer approximations of the 25th, 5th, and 75th percentiles are equal to 12, 15, and 19, respectively.

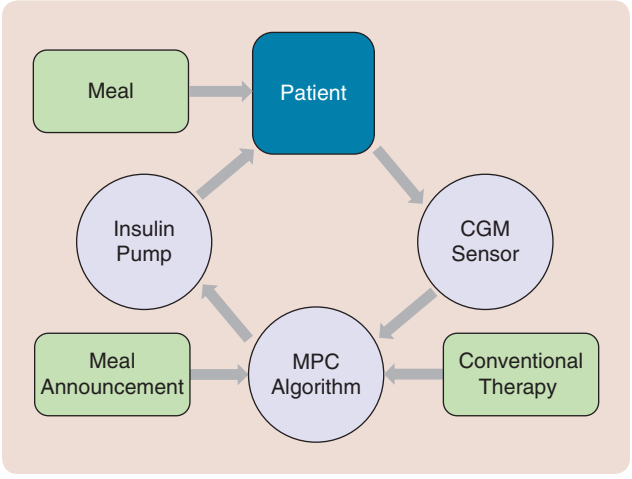

FIGURE 4 A schematic representation of an artificial pancreas. The circled elements represent the main components of the system, which are the continuous glucose monitor (CGM) sensor, the model predictive control (MPC) algorithm, and the subcutaneous insulin pump. The MPC algorithm relies on the patient's conventional therapy and the feedforward action associated with the meal announcement.

The insulin bolus i_B is strictly correlated to the amount of CHO that the patient assumes with the meal and can be represented as an insulin spike that is significantly higher with respect to basal. The insulin bolus calculation is defined as

$$i_B(k) = i_B^{\mathrm{CR}}(k) + \frac{\mathrm{BG}(k) - y_{\mathrm{CF}}}{\mathrm{CF}(k)} - i_{\mathrm{IOB}}^h(k), \tag{9}$$

where the CR-based insulin bolus $i_B^{CR}(k)$ defined in (3) is refined with the addition of two terms. The first term uses one of the parameters included in the conventional therapy

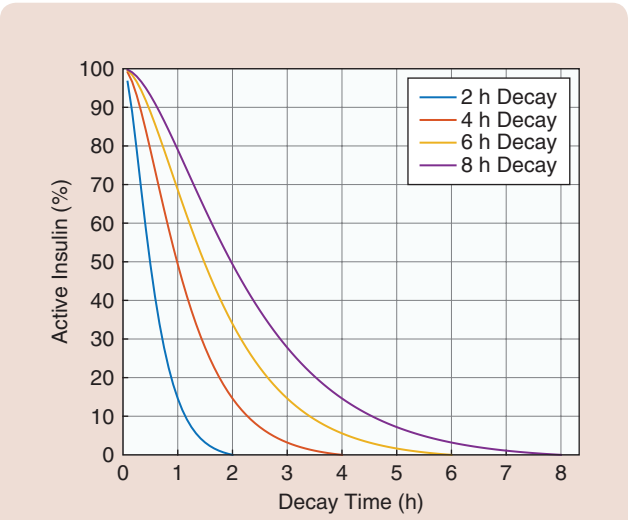

FIGURE 5 Insulin decay curves. Each curve is characterized by a time of decay of h hours, which determines the percentage of still-active insulin as a function of time. The active insulin is the insulin that still has an effect on the patient and is estimated by (10).

[the correction factor (CF)] to adjust the insulin bolus on the basis of the difference between the blood glucose (BG) and a target glucose concentration y_{CF} (mg/dl). BG is usually measured through a fingerstick device, which measures the blood glucose concentration in a drop of blood. The second term reduces the insulin bolus on the basis of the insulin on board (IOB) $i_{\mathrm{IOB}}^h(k)$ (U), which is the estimated residual insulin that still has an effect. IOB is estimated through insulin decay curves [45]

$$\begin{cases} i_{\mathrm{IOB}}^h(k) = 100 \cdot \left(1 - k_a^h \dfrac{f_{\mathrm{IOB}}^h(k)}{k_{\mathrm{den}}^h}\right), \\ f_{\mathrm{IOB}}^h(k) = \dfrac{a_3}{a_1 \cdot (a_1 - a_2)} \left(e^{\frac{-a_1 \cdot k}{k_a^h}} - 1\right) - \dfrac{a_3}{a_2 \cdot (a_1 - a_2)} \left(e^{\frac{-a_2 \cdot k}{k_a^h}} - 1\right), \end{cases} \tag{10}$$

where all the constants are properly chosen on the basis of the time of decay h. The time course of the insulin decay curves for different values of decay is depicted in Figure 5. In the case of adult patients, the decay curve having $h = 4$ h is usually considered to estimate the IOB.

MPC Algorithm Definition

One of the aspects that makes the design of an AP system challenging is the presence of unavoidable delays and inaccuracies in both subcutaneous glucose sensing and insulin delivery. Coping with these issues is particularly difficult when a system disturbance like a meal occurs and triggers a rapid glucose rise that is substantially faster with respect to the time needed in particular for insulin absorption. In the presence of inherent delays, any attempt to increase the responsiveness of the closed-loop system may result in an unstable system behavior and oscillations. A good controller

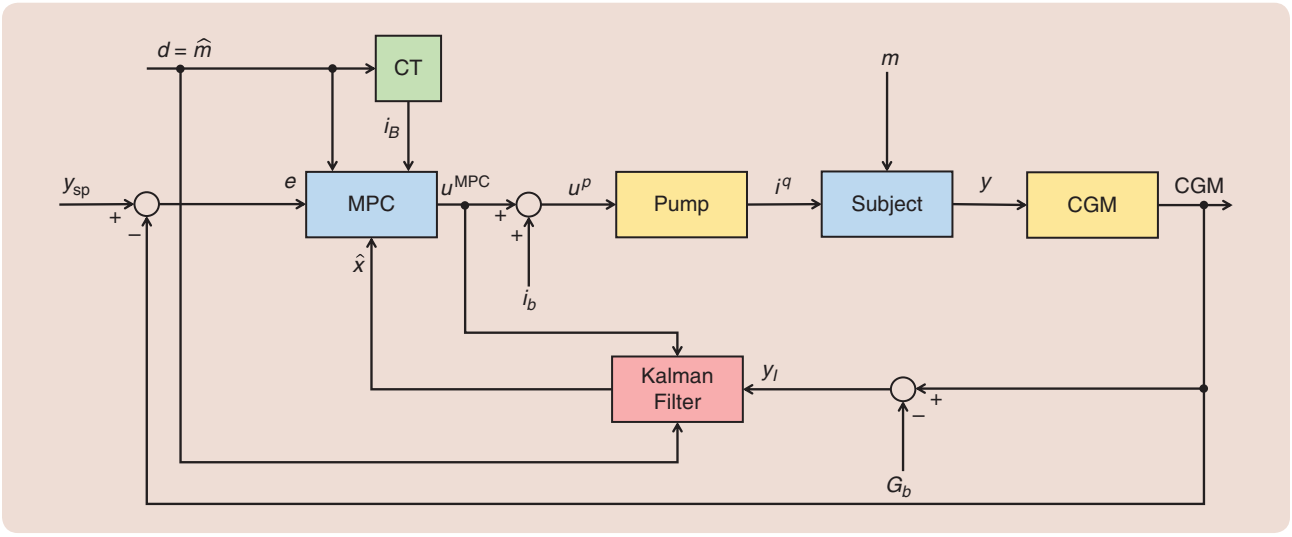

FIGURE 6 A closed-loop scheme implemented in the artificial pancreas system. $d = \hat{m}$ is the estimated quantity of carbohydrates associated with the meal m and is considered in the feedforward action as a disturbance to be rejected. When a meal is announced, model predictive control (MPC) receives the estimation of the nominal insulin bolus i_B through (9), which is included in the conventional therapy (CT). y_{sp} is the glucose setpoint, y is the noisy subcutaneous glucose measured by the continuous glucose monitor (CGM) device, and $e = y_{sp} - CGM$ is the glucose error sent to the MPC. u^{MPC} is the suggested insulin variation with respect to the basal insulin i_b, and u^p is the insulin that has to be infused by the pump, which infuses the quantized insulin i^q into the patient subcutaneous tissue. MPC is also fed with the estimation of the patient state $\hat{x}$, which is estimated through the Kalman filter described in [27]. The latter uses the system inputs and the noisy output $y_l = \text{CGM} - G_b$, with G_b denoting the steady-state glucose concentration during fasting periods (basal glucose).

should consider a relatively slow response; however, a too slow control law could not properly attenuate the postprandial glucose peaks. Thus, the AP system must be designed with a controller able to address the tradeoff between slow and fast regulation [5]. A slow regulation must be considered during quasi-steady-state conditions, like overnight, whereas a fast regulation is useful during postprandial periods where timely insulin infusions are needed.

An MPC for AP is a model-based control approach that uses a model to predict the patient glucose-insulin dynamics. The subcutaneous insulin pump is properly commanded with insulin infusions based on the predicted patient glycemia within a predefined prediction horizon. As shown in Figure 4, the MPC algorithm is enriched with information contained in the patient's conventional therapy and meal announcement, which is a feedforward action activated by the patient at meal times. Meal announcement is used to "inform" the controller that the glycemia is expected to rise rapidly due to a meal, thus requiring prompt insulin delivery. This information is provided to the controller by the glucose prediction computed through the built-in linear model of (2), (7), or (8), which is triggered by the meal announced in the meal input d. The presence of a feedforward action makes the AP system not fully automated. However, meal announcement must be considered as additional knowledge that is available to the patient and should be exploited to improve the postprandial glucose control. In the case of missing a meal announcement, in spite of unavoidable decreases in the control performance, the AP must still operate safely.

Closed-Loop Scheme

The AP closed-loop scheme is shown in Figure 6, where the blue blocks represent the MPC and the patient, the yellow blocks represent the hardware, and the green block represents the conventional therapy used to compute the nominal insulin boluses through (9), which is used in the meal announcement. This scheme is defined on top of the conventional therapy in the sense that the MPC suggests insulin variations with respect to the therapy. During fasting periods, the MPC suggests insulin variations with respect to the patient basal insulin i_b. On the other hand, when a meal is announced, the controller receives information about the nominal insulin bolus i_B and eventually modifies this value based on the estimated state of the patient.

Controller Cost Function and Calibration

The MPC insulin suggestions are driven by the quadratic cost function

$$J(\hat{x}(k|k), u(\cdot), k) = \sum_{i=0}^{N-1} (q(y(k+i) - y_{sp}(k+i) + G_b(k+i))^2 + (u(k+i) - u^0(k+i))^2) + \|x(k+N)\|_P^2, \tag{11}$$

such that

$$\begin{aligned} x(k) &= \hat{x}(k|k), \\ y(k) &= C\hat{x}(k|k), \\ x(k+i+1) &= Ax(k+i) + Bu(k+i) + Md(k+i), \\ y(k+i+1) &= Cx(k+i+1), \\ u^0(k+i) &= i(k+i) - i_b(k+i), \end{aligned}$$

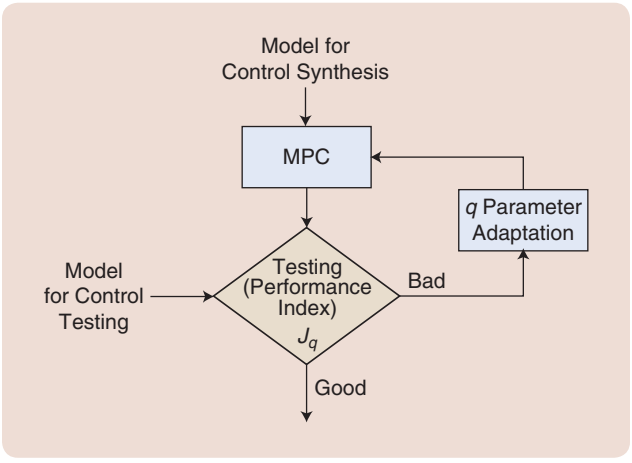

FIGURE 7 A flow chart of the calibration procedure used to tune the parameter q in the cost function (11). The model predictive control (MPC) is synthesized with the model for control synthesis and used in a trial-and-error approach to simulate the closed-loop glucose control on the model for control testing. The process is iterated until the decrease on the performance index J_q, defined in (12), becomes negligible.

where $\hat{x}(k|k)$ is the state estimated through the Kalman filter described in [27] at time k, u^0 is the variation of the insulin suggested by the conventional therapy with respect to the basal insulin i_b, y_{sp} (mg/dl) is the desired glucose setpoint, N is the prediction horizon, $q > 0$ is a tunable parameter, and P is the unique nonnegative solution of the discrete time Riccati equation (S5). The matrices A, B, C, and M define the linear glucose-insulin model used to predict the patient glycemia within the horizon N. Any linear model having the form of (2) can be included in the cost function or, alternatively, the identified models (7) or (8) can be considered, thus defining an individualized controller.

The cost to be minimized includes the glucose setpoint and the conventional therapy y_{sp} and u^0, respectively. The insulin suggestion is calculated by computing the optimal tradeoff between the glucose error with respect to the setpoint and the insulin variations with respect to the conventional therapy. The tradeoff is defined through the parameter q. Higher q values are associated with a higher cost to the glucose variations, thus resulting in a more aggressive controller that strives for maintaining the glycemia at the setpoint. On the other hand, lower q values are associated with a higher cost to the insulin variations with respect to the conventional therapy, resulting in a more conservative controller.

The q value must be set on the basis of the estimated IS of the patient. Patients who are more insulin sensitive require a more conservative controller, whereas patients characterized by elevated insulin resistance require more aggressive insulin administrations. The tuning of q is handled through a calibration procedure that is performed in simulation, by considering a trial and error approach driven by the performance index

$$J_q(q) = \sqrt{X_{\mathrm{CVGA}}^2 + Y_{\mathrm{CVGA}}^2} + k_1^{\mathrm{C}} \cdot (\log_{10}(q) - k_2^{\mathrm{C}})^2, \qquad (12)$$

where X_{CVGA} and Y_{CVGA} are the coordinates achieved in simulation in the control variability grid analysis (CVGA) defined in [20] and [46], and k_1^{C} and k_2^{C} are tunable parameters. The CVGA coordinates are obtained by simulating a predefined calibration scenario, and the process is repeated until the minimum cost J_q is found. The flow chart representing the calibration procedure is shown in Figure 7. A linear model for control synthesis is used to synthesize the MPC that simulates the closed-loop control on a model for control testing. At the end of each simulation, the performance index (12) is evaluated, and the process is repeated until the decrease of the performance index becomes negligible, thus resulting in the calibrated q value

$$\hat{q} = \min\{\max\{\mathrm{argmin}_q\{J_q(q)\}, \bar{q}_l\}, \bar{q}_h\},$$

where $\bar{q}_l$ and $\bar{q}_h$ are minimum and maximum safety thresholds, respectively.

In the case of individualized models, the model for control testing is the same model used for control synthesis. This procedure is feasible in a real scenario, where the identified model would be used for the trial-and-error approach, and the real patient would be equipped with the controller including the resulting calibrated $\hat{q}$. In the case of MPC based on nonindividualized models, the calibration procedure is repeated for each virtual subject, which is characterized by (1), considered as the model for control testing. The regression model $\hat{q}(BW, CR) = e^{r_1 \cdot BW + r_2 \cdot CR + r_{int}}$ is then used to adapt the q value to each patient on the basis of his/her CR and body weight. As described in [27], the

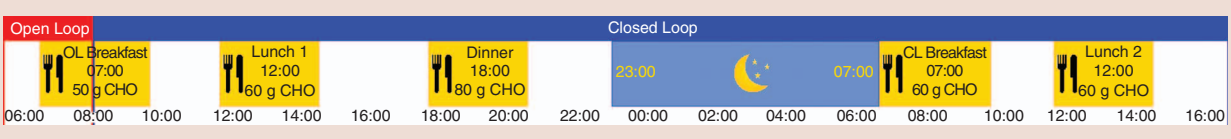

FIGURE 8 A scenario used for closed-loop (CL) simulations. The scenario starts at 6:00 and lasts 34 h, and the loop is closed at 8:00. The first breakfast is compensated in open loop (OL) through the conventional therapy, while the remaining meals are compensated in CL. The night starts at 23:00 and lasts 8 h. Meal amounts are 50 g of carbohydrates (CHO) for the first breakfast, 80-g CHO for the dinner, and 60-g CHO for the remaining meals.

TABLE 3 Closed-loop performance indices achieved by nonindividualized model predictive control (L-MPC), insulin-to-carbo ratio MPC (CR-MPC), nonparametric MPC (NP-MPC), and constrained optimization MPC (CO-MPC) in the simulation scenario of Figure 8. O is the overall scenario, N is night, and PP are closed-loop postprandial periods. The † symbol denotes the p-values significance.

		O	N	PP
A (mg/dl)	L-MPC	144.85 (126.81, 158.88)	121.75 (113.90, 127.70)	155.83 (29.85)
	CR-MPC	144.10 (126.47, 155.66) ††	122.07 (113.98, 127.78) ††	154.13 (26.76) ††
	NP-MPC	133.34 (118.73, 145.23) †††	114.57 (108.30, 119.36) †††	144.88 (26.17) †††
	CO-MPC	136.95 (123.97, 148.12) †††	116.03 (110.73, 122.56) †††	152.24 (26.01) †
SD (mg/dl)	L-MPC	21.41 (17.18, 27.45)	6.68 (4.35, 10.47)	19.95 (15.95, 25.13)
	CR-MPC	21.50 (16.63, 26.77) †††	6.25 (3.99, 9.04) †††	19.72 (15.79, 24.69)
	NP-MPC	22.11 (17.96, 27.46)	5.04 (3.09, 7.24) †††	21.41 (18.52, 25.91) †††
	CO-MPC	22.66 (18.85, 29.01) ††	5.50 (3.74, 8.06) ††	22.35 (18.54, 26.93) †††
CV (mg/dl)	L-MPC	0.16 (0.13, 0.19)	0.06 (0.04, 0.08)	0.13 (0.05)
	CR-MPC	0.16 (0.13, 0.18) ††	0.05 (0.03, 0.08) †	0.13 (0.05)
	NP-MPC	0.17 (0.14, 0.21) †††	0.04 (0.03, 0.06) ††	0.16 (0.05) †††
	CO-MPC	0.17 (0.14, 0.20) †††	0.05 (0.03, 0.07) †	0.16 (0.05) †††
Tt (%)	L-MPC	95.18 (75.66, 100.00)	100.00 (100.00, 100.00)	90.57 (57.86, 100.00)
	CR-MPC	95.65 (81.23, 100.00) †	100.00 (100.00, 100.00)	91.72 (66.61, 100.00) †
	NP-MPC	97.37 (87.95, 100.00) †††	100.00 (100.00, 100.00)	95.16 (78.96, 100.00) †††
	CO-MPC	95.24 (82.25, 100.00)	100.00 (100.00, 100.00)	90.47 (69.11, 100.00)
Ttt (%)	L-MPC	46.17 (24.98)	100.00 (87.89, 100.00)	16.93 (6.61, 66.82)
	CR-MPC	48.70 (24.41) †	100.00 (91.23, 100.00) †	26.51 (8.39, 66.77) †
	NP-MPC	65.17 (21.07) †††	100.00 (100.00, 100.00) †††	45.83 (22.81, 70.42) †††
	CO-MPC	59.36 (23.68) †††	100.00 (100.00, 100.00) †	35.26 (15.36, 62.34) ††
Ta (%)	L-MPC	4.35 (0.00, 24.34)	0.00 (0.00, 0.00)	8.02 (0.00, 42.14)
	CR-MPC	3.67 (0.00, 18.77) †	0.00 (0.00, 0.00)	6.41 (0.00, 33.13) †
	NP-MPC	1.67 (0.00, 12.05) †††	0.00 (0.00, 0.00)	3.33 (0.00, 20.05) †††
	CO-MPC	4.35 (0.00, 17.75)	0.00 (0.00, 0.00)	8.70 (0.00, 30.89)
Tb (%)	L-MPC	0.00 (0.00, 0.00)	0.00 (0.00, 0.00)	0.00 (0.00, 0.00)
	CR-MPC	0.00 (0.00, 0.00)	0.00 (0.00, 0.00)	0.00 (0.00, 0.00)
	NP-MPC	0.00 (0.00, 0.00)	0.00 (0.00, 0.00)	0.00 (0.00, 0.00)
	CO-MPC	0.00 (0.00, 0.00)	0.00 (0.00, 0.00)	0.00 (0.00, 0.00)
#ht	L-MPC	9	0	9
	CR-MPC	18	0	18
	NP-MPC	18	0	15
	CO-MPC	2	0	2
Number of patients with ht	L-MPC	4	0	4
	CR-MPC	4	0	4
	NP-MPC	5	0	5
	CO-MPC	1	0	1

(*continued*)

TABLE 3 Closed-loop performance indices achieved by nonindividualized model predictive control (L-MPC), insulin-to-carbo ratio MPC (CR-MPC), nonparametric MPC (NP-MPC), and constrained optimization MPC (CO-MPC) in the simulation scenario of Figure 8. O is the overall scenario, N is night, and PP are closed-loop postprandial periods. The † symbol denotes the p-values significance. (*Continued*)

		O	N	PP
Daily insulin needs (U)	L-MPC	47.35 (39.15, 59.08)	9.35 (8.06, 10.92)	46.29 (35.39, 53.52)
	CR-MPC	49.75 (39.50, 62.90)†††	9.68 (7.99, 10.91)	48.49 (36.28, 59.36)††
	NP-MPC	51.18 (41.10, 63.55)††	10.09 (8.46, 12.10)†††	44.39 (36.01, 56.77)
	CO-MPC	42.70 (36.63, 51.70)†††	9.35 (8.01, 11.24)	36.52 (31.07, 45.74)†††
Daily insulin needs per kg (U/kg)	L-MPC	0.69 (0.59, 0.86)	0.14 (0.12, 0.17)	0.65 (0.53, 0.83)
	CR-MPC	0.76 (0.60, 0.92)†††	0.14 (0.12, 0.17)	0.70 (0.54, 0.85)†††
	NP-MPC	0.76 (0.61, 0.95)††	0.14 (0.12, 0.18)†††	0.67 (0.52, 0.86)
	CO-MPC	0.62 (0.52, 0.76)†††	0.14 (0.11, 0.17)	0.53 (0.44, 0.69)†††

parameters r_1, r_2, and r_{int} were obtained by relying on 100 calibrated $\hat{q}$ associated with the entire adult virtual population of the UVA/Padova simulator.

SIMULATION RESULTS

The MPC considered in simulation is entirely defined in [27]. The MPC is equipped with properly defined insulin constraints and driven by the cost function (11). For an estimation of the MPC behavior in a real scenario, the simulations were performed on the 100 nonlinear, time-variant, adult virtual subjects of the UVA/Padova simulator [35]. Furthermore, to test the controller safety and robustness, the IS of each virtual subject was randomly varied by a ±25% factor, and the controller was blind to these variations.

The simulation scenario is shown in Figure 8 and includes five meals, of which the first is compensated in open loop (through the conventional therapy), while the remaining meals are compensated for through the MPC. The simulation scenario starts at 6:00 and lasts 34 h, and the loop is closed at 8:00. Note that the loop is closed within the postprandial period of the open-loop compensated meal, increasing the variability associated with the closed-loop starting conditions. Meal amounts are 50-g CHO for the first breakfast, 60-g CHO for the second one, 60-g CHO for the two lunches, and 80-g CHO for the dinner. Postprandial periods are defined as 4-h time intervals starting from each meal time. Night period starts at 23:00 and lasts 8 h.

The glucose control performance is evaluated through standard indices in evaluating AP clinical trials [47]. The considered metrics are the following: average glucose (A), glucose standard deviation (SD), glucose coefficient of variation (CV), time in target or percentage of time spent within 70–180 mg/dl (Tt), time in tight target or percentage of time spent within 70–140 mg/dl (Ttt), time above target or percentage of time spent above 180 mg/dl (Ta), time below target or percentage of time spent below 70 mg/dl (Tb), number of hypotreatments (#ht), and number of patients with at least one hypotreatment (# patients with ht). A hypotreatment consists of 16-g CHO that are administered in case the patient glycemia falls below 65 mg/dl. This process is automatically performed in the simulation environment with a constraint that imposes a time gap of at least 30 min between two consecutive hypotreatments. In addition, insulin metrics are also included in terms of daily insulin needs (measured in insulin units U) and daily insulin needs normalized by the patient weight (U/kg).

Table 3 shows the outcome indices achieved through the linearized nonindividualized MPC (L-MPC), customized MPC based on the CR-based models (CR-MPC), individualized MPCs synthesized by considering the NP models (NP-MPC), and the models identified through CO (CO-MPC). Both NP-MPC and CO-MPC were synthesized based on individualized models identified from historical input–output data generated in silico by following the identification scenarios described in [41]. Each index is evaluated during the overall scenario (O), during the night (N), and within the closed-loop postprandial periods (PP). Nonnormal data are shown as median (25th percentile and 75th percentile), whereas normal data are shown as mean (standard deviation). Given that all the Tb percentiles of Table 3 are equal to zero, to perform a quantitative comparison, Table 4 shows the Tb indices in terms of mean (standard deviation). Statistical comparisons are performed between L-MPC and the customized MPCs with the following significance levels:

$$p-\text{value}(p)\ \text{significance level} = \begin{cases} \dagger & p < 0.05, \\ \dagger\dagger & p < 0.01, \\ \dagger\dagger\dagger & p < 0.001, \end{cases}$$

where p is evaluated with the paired t-test for normally distributed data and the Wilcoxon signed-rank test otherwise. The test of normality is performed through the Lilliefors test.

In this article, CR-MPC, NP-MPC, and CO-MPC are referred to as individualized MPCs. The individualized MPCs significantly reduced the average glucose. The reduction is more noticeable with NP-MPC and CO-MPC, which are synthesized on patient-individualized glucose-insulin models. Although the achieved time in target is numerically similar to all of the considered controllers, the individualized MPCs significantly increased the time in tight target and reduced the time above target without increasing the time below target. The reduction of hyperglycemia was also significant with the exception of CO-MPC, which used a significantly lower amount of insulin with respect to the other controllers and encountered only two hypotreatments in a single patient within the entire adult virtual population. Thus, it is possible to conclude that the individualized MPCs are able to better maintain steadier the glucose concentration without significantly increasing the risk of hyper- or hypoglycemia.

Glucose control is particularly challenging within the postprandial periods, where the rapid increase of glucose induced by a meal must be promptly compensated for by taking into account the risk of induced postprandial hypoglycemia. As shown in Figure 9, the postprandial glucose compensation is slightly improved with CR-MPC with respect to L-MPC, since the glucose peaks are lower and the glucose decrease is faster. However, these controllers are characterized by a conservative behavior at the end of each postprandial period, where the glycemia decrease is systematically slowed down before reaching the glucose setpoint (120 mg/dl). This conservative compensation was introduced to minimize the risk of postprandial hypoglycemia, which is caused by insulin overestimation for meal compensation and would require a hypotreatment to restore the proper glucose concentration. Thanks to the availability of patient-individualized models, this behavior is no longer noticeable in NP-MPC and CO-MPC, which can rely on more effective glucose predictions. Thus, both the controllers based

TABLE 4 The mean and standard deviation of the time below target achieved in closed loop by nonindividualized model predictive control (L-MPC), insulin-to-carbo ratio MPC (CR-MPC), nonparametric MPC (NP-MPC), and constrained optimization MPC (CO-MPC) in the simulation scenario of Figure 8. O is the overall scenario, N is night, and PP are closed-loop postprandial periods.

		O	N	PP
Tb (%)	L-MPC	0.17 (0.80)	0.00 (0.00)	0.33 (1.61)
	CR-MPC	0.27 (1.51)	0.00 (0.00)	0.53 (3.02)
	NP-MPC	0.30 (1.35)	0.00 (0.00)	0.41 (2.29)
	CO-MPC	0.08 (0.56)	0.00 (0.00)	0.13 (1.06)

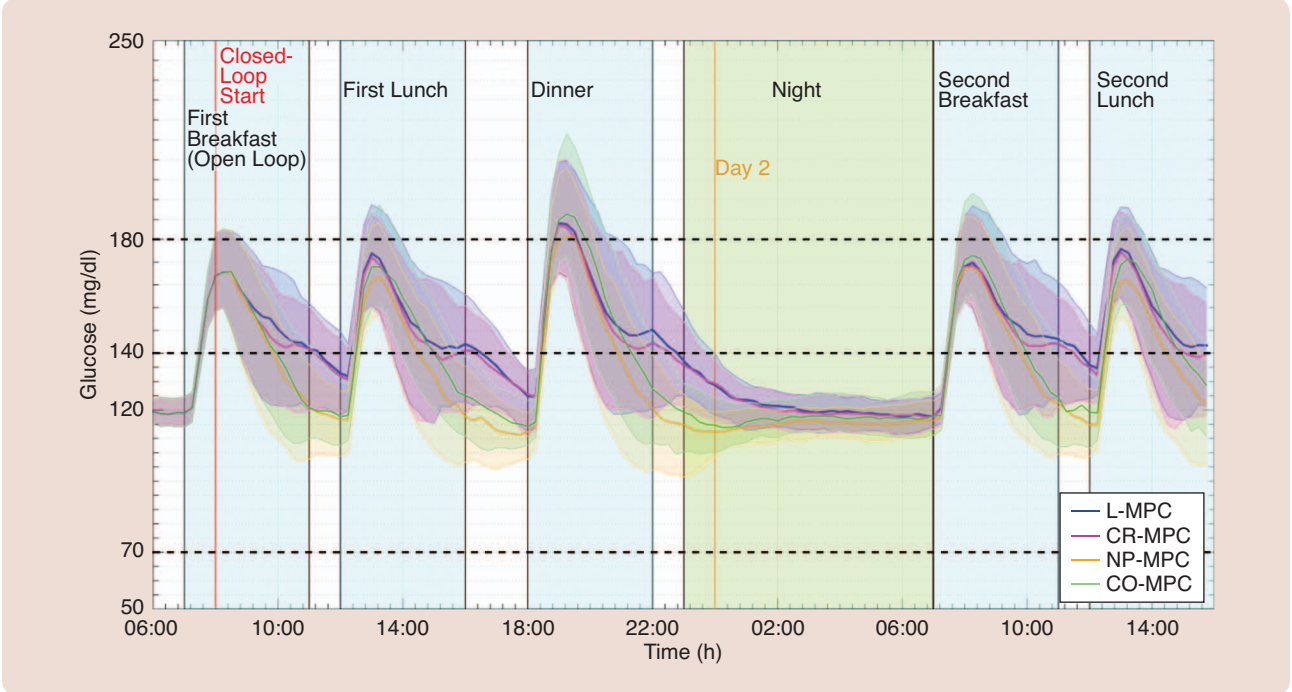

FIGURE 9 The blood glucose concentration achieved by the linearized nonindividualized model predictive control (L-MPC), customized MPC synthesized with the insulin-to-carbo ratio-based (CR-MPC) models, individualized MPC synthesized by considering the nonparametric (NP-MPC), and the constrained optimization (CO-MPC) models in the simulation scenario of Figure 8. Glucose values are shown in terms of the median (solid lines) surrounded by colored regions representing the glucose 25th and 75th percentiles.

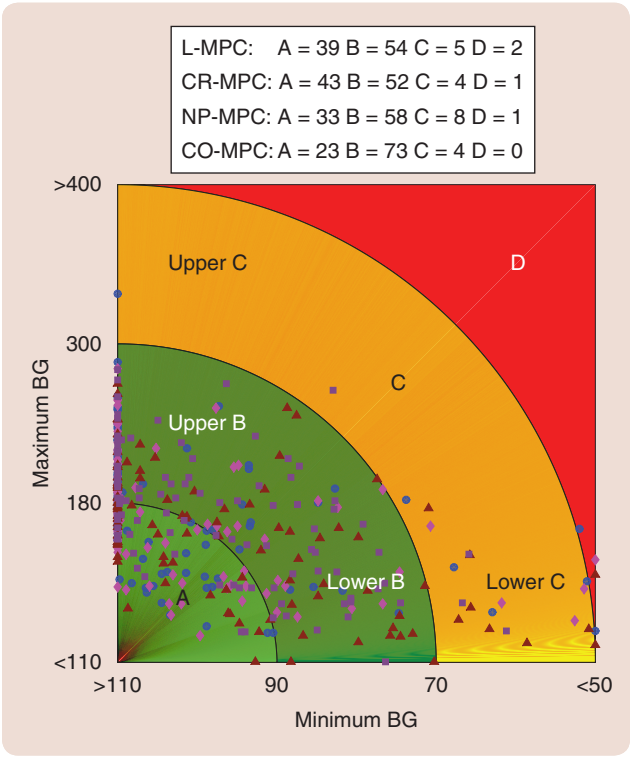

FIGURE 10 A control variability grid analysis [20] achieved by the linearized nonindividualized model predictive control (L-MPC, blue circles), customized MPC synthesized with the insulin-to-carbo ratio based (CR-MPC, magenta diamonds) models, individualized MPC synthesized by considering the nonparametric (NP-MPC, brown triangles), and constrained optimization (CO-MPC, violet squares) models in the simulation scenario of Figure 8. Each point represents the combination of the minimum and maximum blood glucose (BG) reached by a virtual subject in simulation.

on patient-individualized models are able to faster compensate for the postprandial glycemia and reach the glucose setpoint without slowing down the glycemia decrease for safety purposes. In particular, CO-MPC is able to quickly compensate for the postprandial glycemia without creating glucose undershoots before reaching the setpoint. This behavior is evident in Figure 9, where the shadowed region representing the glucose variability of CO-MPC is narrower with respect to NP-MPC.

The faster glucose compensation of NP-MPC and CO-MPC significantly increases the postprandial SD and CV, as shown in Table 3, consequently increasing the same indices in the overall scenario. However, as shown in the CVGA of Figure 10, this does not translate into a worsening of the overall control performance. Each point in the CVGA represents the combination of the minimum and maximum glycemia reached by each patient during a simulation. A point is present for each patient for each one of the four considered MPCs, thus resulting in 400 points. Although the number of points in the A region is reduced with NP-MPC and CO-MPC, their scatter plots are within the A and B regions, denoting that the overall glucose control performance is not compromised. Moreover, CO-MPC results in 96 points included in the A and B regions and no points in the D region, thus achieving the best performance in terms of CVGA.

CONCLUSION

Despite the continuous efforts devoted to AP development in the last decades, an AP system is not yet available on the market. One of the major issues involves the intersubject variability affecting T1D patients, which makes the definition of a single controller suitable for any patient practically impossible. Moreover, a state-of-the-art, noninvasive, and portable AP system is composed of subcutaneous hardware components, and the control algorithm must be properly designed to reside on a standalone device with limited battery life and computational power. These characteristics make the design of a safe and effective AP system even more challenging, due to the inherent delays affecting the subcutaneous insulin delivery route and the tradeoff between control performance and computational power expenditure.

As a result of the MPC's ability to address inherent delays of the process under control, it is one of the most promising control approaches in the context of an AP. However, the achievable control performance is strictly related to the prediction capabilities of the model included in the controller, which, in general, can be highly nonlinear. The currently used MPC in clinical experiments relies on a linear average glucose-insulin model designed to represent the average dynamics of a subject with diabetes. This nonindividualized MPC is not designed to cope with patient-specific dynamics but is designed to be noncomputationally demanding and robust enough to result in a safe and effective control law.

The introduction of patient-tailored, glucose-insulin linear models opens possibilities for designing individualized MPCs capable of significantly improving the achievable glucose control performance and enhancing the AP system safety and efficacy without increasing the computational complexity of the control algorithm. The closed-loop simulations have shown that the individualized MPCs are able to address the intersubject variability and are particularly effective within the postprandial periods, where the patient glycemia is substantially perturbed and the controller needs to react promptly to compensate for the glucose rise without inducing postprandial hypoglycemia.

The proposed individualization approaches don't address intrasubject variability (which represents the variability characterizing a specific patient over time). Future investigation both in silico and in vivo will need to take this variability into account. However, to achieve preliminary clinical results on the safety and feasibility of the proposed identification approaches, future works will consider the identification of individualized glucose-insulin models from clinical data of patients with T1D. Clinical studies will have to be

designed to sufficiently achieve perturbed clinical data for model identification. As described in [41], one of the major issues associated with model individualization is the identifiability of glucose-insulin dynamics. The CO approach is preferable with respect to the NP, since it identifies linear compartmental models having a fixed structure and requires a shorter identification data set that would be more easily realizable in a real scenario. Thus, individualized MPCs usable in clinical trials will be synthesized, having the potential of further improving the clinical results and making a significant step toward the design of an AP suitable for the market.

AUTHOR INFORMATION

Mirko Messori (mirko.messori01@ateneopv.it) obtained the master's degree (cum laude) in computer science with specialization in automation in 2012 and the Ph.D. degree in electronics, computer science, and electrical engineering in 2016, both from the University of Pavia, Italy. Since then, he has been with the Identification and Control Systems Laboratory of the University of Pavia as a postdoctoral fellow. The main topics of his research cover several identification and control techniques of linear and nonlinear systems and both supervised and unsupervised machine learning techniques.

Gian Paolo Incremona received the master's degree (cum laude) in electric engineering in 2012 and the Ph.D. degree in electronics, computer science, and electrical engineering in 2016, both from the University of Pavia, Italy. Since then, he has been with the Identification and Control Systems Lab of the University of Pavia as a postdoctoral fellow. Since June 2017, he has been an assistant professor of automatic control at Politecnico di Milano, and his research interests include industrial robotics, real-time physical systems, optimal control, and variable structure control methods of the sliding mode type.

Claudio Cobelli is emeritus professor of biomedical engineering at the University of Padova, Italy. His research is in the modeling and control of metabolic-endocrine systems, supported by NIH, JDRF, and EU. He published 519 papers in refereed journals, is the coauthor of eight books, and holds ten patents with an h-index of 94. He is an associate editor of *IEEE Transactions on Biomedical Engineering* and *Journal of Diabetes Science and Technology*, and he serves on the editorial boards of *Medical and Biological Engineering* and *Diabetes, Technology and Therapeutics*. In 2010, he received the Diabetes Technology Artificial Pancreas Research Award. He is a Fellow of the IEEE European Alliance for Medical and Biological Engineering and Science.

Lalo Magni received the master's degree in 1994 and the Ph.D. degree in 1998, both from the University of Pavia, Italy. Since that time, he has been with the University of Pavia where he is now full professor of automatic control and dean of Engineering Faculty. His current research interests include nonlinear control, predictive control, robust control, process control, and the artificial pancreas.

REFERENCES

[1] C. Cobelli, E. Renard, and B. P. Kovatchev, "Artificial pancreas: Past, present, future," *Diabetes*, vol. 60, no. 11, pp. 2672–2682, 2011.

[2] G. M. Steil, K. Rebrin, C. Darwin, F. Hariri, and M. F. Saad, "Feasibility of automating insulin delivery for the treatment of type 1 diabetes," *Diabetes*, vol. 55, no. 12, pp. 3344–3350, 2006.

[3] M. Messori, C. Cobelli, and L. Magni, "Artificial pancreas: From in-silico to in-vivo," in *Proc. IFAC 9th Int. Symp. Advanced Control of Chemical Processes*, Whistler, British Columbia, Canada, June 7–10, 2015, pp. 1301–1309.

[4] B. W. Bequette, "Challenges and recent progress in the development of a closed-loop artificial pancreas," *Annu. Rev. Control*, vol. 36, no. 2, pp. 255–266, 2012.

[5] C. Cobelli, C. Dalla Man, G. Sparacino, L. Magni, G. De Nicolao, and B. P. Kovatchev, "Diabetes: Models, signals, and control," *IEEE Rev. Biomed. Eng.*, vol. 2, pp. 54–96, 2009. doi: 10.1109/RBME.2009.2036073.

[6] F. H. El-Khatib, S. J. Russell, D. M. Nathan, R. G. Sutherlin, and E. R. Damiano, "A bihormonal closed-loop artificial pancreas for type 1 diabetes," *Sci. Transl. Med.*, vol. 2, no. 27, pp. 27ra27, 2010.

[7] R. Hovorka, J. M. Allen, D. Elleri, L. J. Chassin, J. Harris, D. Xing, C. Kollman, T. Hovorka, A. M. F. Larsen, M. Nodale, A. De Palma, M. E. Wilinska, C. L. Acerini, and D. B. Dunger, "Manual closed-loop insulin delivery in children and adolescent with type 1 diabetes: A phase 2 randomised crossover trial," *Lancet*, vol. 375, no. 9716, pp. 743–751, 2010.

[8] S. A. Weinzimer, G. M. Steil, K. L. Swan, J. Dziura, N. Kurtz, and W. V. Tamborlane, "Fully-automated closed-loop insulin delivery versus semi-automated hybrid control in pediatric patients with type 1 diabetes using an artificial pancreas," *Diabetes Care*, vol. 31, no. 5, pp. 934–939, 2008.

[9] R. Hovorka, "Closed-loop insulin delivery: From bench to clinical practice," *Nat. Rev. Endocrinol.*, vol. 7, no. 7, pp. 385–395, 2011.

[10] M. Breton, A. Farret, D. Bruttomesso, S. Anderson, L. Magni, S. Patek, C. Dalla Man, J. Place, S. Demartini, S. Del Favero, C. Toffanin, C. Hughes-Karvetski, E. Dassau, H. Zisser, F. J. Doyle III, G. De Nicolao, A. Avogaro, C. Cobelli, E. Renard, and B. Kovatchev, on behalf of the International Artificial Pancreas (iAP) Study Group, "Fully integrated artificial pancreas in type 1 diabetes: Modular closed-loop glucose control maintains near normoglycemia," *Diabetes*, vol. 61, no. 9, pp. 2230–2237, 2012.

[11] F. J. Doyle, L. M. Huyett, J. B. Lee, H. C. Zisser, and E. Dassau, "Closed-loop artificial pancreas systems: Engineering the algorithms," *Diabetes Care*, vol. 37, no. 5, pp. 1191–1197, 2014.

[12] S. J. Russell, F. H. El-Khatib, M. Sinha, K. L. Magyar, K. McKeon, L. G. Goergen, C. Balliro, M. A. Hillard, D. M. Nathan, and E. R. Damiano, "Outpatient glycemic control with a bionic pancreas in type 1 diabetes," *N. Engl. J. Med.*, vol. 371, pp. 313–325, 2014. doi: 10.1056/NEJMoa1314474.

[13] S. Del Favero, J. Place, J. Kropff, M. Messori, P. Keith-Hynes, R. Visentin, M. Munaro, D. Bruttomesso, S. Galasso, F. Boscari, C. Toffanin, F. Di Palma, G. Lanzola, S. Scarpellini, A. Ferret, B. Kovatchev, L. Magni, A. Avogaro, J. H. DeVries, C. Cobelli, and E. Renard, on behalf of the AP@home Consortium, "Multicentre outpatient dinner/overnight reduction of hypoglycemia and increased time of glucose in target with a wearable artificial pancreas using multi-modular model predictive control algorithm in adults with type 1 diabetes," *Diabetes Obesity Metab.*, vol. 17, no. 5, pp. 468–476, 2015.

[14] H. Thabit, A. Lubina-Solomon, M. Stadler, L. Leelarathna, E. Walkinshaw, A. Pernet, J. M. Allen, A. Iqbal, P. Choudhary, K. Kumareswaran, M. Nodale, C. Nisbet, M. E. Wilinska, K. D. Barnard, D. B. Dunger, S. R. Heller, S. A. Amiel, M. L. Evans, and R. Hovorka, "Home use of closed-loop insulin delivery for overnight glucose control in adults with type 1 diabetes: A 4-week, multicentre, randomised crossover study," *Lancet Diabetes Endocrinol.*, vol. 2, no. 9, pp. 701–709, 2014.

[15] J. Kropff, S. Del Favero, J. Place, C. Toffanin, R. Visentin, M. Monaro, M. Messori, F. D. Palma, G. Lanzola, A. Farret, F. Boscari, S. Galasso, P. Magni, A. Avogaro, P. Keith-Hynes, B. P. Kovatchev, D. Bruttomesso, C. Cobelli, J. H. DeVries, E. Renard, and L. Magni, for the AP@home Consortium, "2 month evening and night closed-loop glucose control in patients with type 1 diabetes under free-living conditions: A randomised crossover trial," *Lancet Diabetes Endocrinol.*, vol. 3, no. 12, pp. 939–947, 2015.

[16] L. Magni, D. M. Raimondo, L. Bossi, C. Dalla Man, G. De Nicolao, B. Kovatchev, and C. Cobelli, "Model predictive control of type 1 diabetes: An in silico trial," *J. Diabetes Sci. Technol.*, vol. 1, no. 6, pp. 804–812, 2007.

[17] M. E. Wilinska, E. S. Budiman, M. B. Taub, D. Elleri, J. M. Allen, C. L. Acerini, D. B. Dunger, and R. Hovorka, "Overnight closed-loop insulin delivery with model predictive control: Assessment of hypoglycemia and hyperglycemia risk using simulation studies," *J. Diabetes Sci. Technol.*, vol. 3, no. 5, pp. 1109–1120, 2009.
[18] B. Grosman, E. Dassau, H. C. Zisser, L. Jovanovic, and F. J. Doyle, III, "Zone model predictive control: A strategy to minimize hyper- and hypoglycemic events," *J. Diabetes Sci. Technol.*, vol. 4, no. 4, pp. 961–975, 2010.
[19] S. D. Patek, L. Magni, E. Dassau, C. Hughes-Karvetski, C. Toffanin, G. De Nicolao, S. Del Favero, M. Breton, C. Dalla Man, E. Renard, H. Zisser, F. J. Doyle, C. Cobelli, and B. P. Kovatchev, "Modular closed-loop control of diabetes," *IEEE Trans. Biomed. Eng.*, vol. 59, no. 11, pp. 2986–2999, 2012.
[20] P. Soru, G. D. Nicolao, C. Toffanin, C. Dalla Man, C. Cobelli, and L. Magni, on behalf of the AP@home Consortium, "MPC based artificial pancreas: Strategies for individualization and meal compensation," *Annu. Rev. Control*, vol. 36, no. 1, pp. 118–128, 2012.
[21] B. P. Kovatchev, C. Cobelli, E. Renard, S. Anderson, M. Breton, S. Patek, W. Clarke, D. Bruttomesso, A. Maran, S. Costa, A. Avogaro, C. Dalla Man, A. Facchinetti, L. Magni, G. De Nicolao, J. Place, and A. Farret, "Multinational study of subcutaneous model-predictive closed-loop control in type 1 diabetes mellitus: Summary of the results," *J. Diabetes Sci. Technol.*, vol. 4, no. 6, pp. 1374–1381, 2010.
[22] R. Hovorka, K. Kumareswaran, J. Harris, J. M. Allen, D. Elleri, D. Xing, C. Kollman, M. Nodale, H. R. Murphy, D. B. Dunger, S. A. Amiel, S. R. Heller, M. E. Wilinska, and M. L. Evans. (2011). Overnight closed loop insulin delivery (artificial pancreas) in adults with type 1 diabetes: Crossover randomised controlled studies, *Br. Med. J.* [Online]. Available: http://dx.doi.org/10.1136/bmj.d1855
[23] E. Dassau, H. Zisser, R. A. Harvey, M. W. Percival, B. Grosman, W. Bevier, E. Atlas, S. Miller, R. Nimri, L. Jovanovic, and F. J. Doyle, III, "Clinical evaluation of a personalized artificial pancreas," *Diabetes Care*, vol. 36, no. 4, pp. 801–809, 2013.
[24] H. Zisser, E. Renard, B. Kovatchev, C. Cobelli, A. Avogaro, R. Nimri, L. Magni, B. Buckingham, H. P. Chase, F. J. Doyle, III, J. Lum, P. Calhoun, C. Kollman, E. Dassau, A. Farret, J. Place, M. Breton, S. Anderson, C. Dalla Man, S. Del Favero, D. Bruttomesso, A. Filippi, R. Scotton, M. Phillip, E. Atlas, I. Muller, S. Miller, C. Toffanin, D. M. Raimondo, G. De Nicolao, and R. W. Beck, for the Control to Range Study Group, "Multicenter closed-loop insulin delivery study points to challenges for keeping blood glucose in a safe range by a control algorithm in adults and adolescents with type 1 diabetes from various sites," *Diabetes Technol. Therapeut.*, vol. 16, no. 10, pp. 613–622, 2014.
[25] H. P. Chase, F. J. Doyle, III, H. Zisser, E. Renard, R. Nimri, C. Cobelli, B. A. Buckingham, D. M. Maahs, S. Anderson, L. Magni, J. Lum, P. Calhoun, C. Kollman, and R. W. Beck, for the Control to Range Study Group. "Multicenter closed-loop/hybrid meal bolus insulin delivery with type 1 diabetes," *Diabetes Technol. Therapeut.*, vol. 16, no. 10, pp. 623–632, 2014.
[26] Y. M. Luijf, J. H. DeVries, K. Zwinderman, L. Leelarathna, M. Nodale, K. Caldwell, K. Kumareswaran, D. Elleri, J. M. Allen, M. E. Wilinska, M. L. Evans, R. Hovorka, W. Doll, M. Ellmerer, J. K. Mader, E. Renard, J. Place, A. Farret, C. Cobelli, S. Del Favero, C. Dalla Man, A. Avogaro, D. Bruttomesso, A. Filippi, R. Scotton, L. Magni, G. Lanzola, F. Di Palma, P. Soru, C. Toffanin, G. De Nicolao, S. Arnolds, C. Benesch, and L. Heinemann, "Day and night closed-loop control in adults with type 1 diabetes mellitus: A comparison of two closed-loop algorithms driving continuous subcutaneous insulin infusion versus patient self-management," *Diabetes Care*, vol. 36, no. 12, pp. 3882–3887, 2013.
[27] C. Toffanin, M. Messori, F. Di Palma, G. De Nicolao, C. Cobelli, and L. Magni, "Artificial pancreas: Model predictive control design from clinical experience," *J. Diabetes Sci. Technol.*, vol. 7, no. 6, pp. 1470–1483, 2013.
[28] B. P. Kovatchev, E. Renard, C. Cobelli, H. C. Zisser, P. Keith-Hynes, S. M. Anderson, S. A. Brown, D. R. Chernavvsky, M. D. Breton, L. B. Mize, A. Farret, J. Place, D. Bruttomesso, S. Del Favero, F. Boscari, S. Galasso, A. Avogaro, L. Magni, F. D. Palma, C. Toffanin, M. Messori, E. Dassau, and F. J. Doyle, III, "Safety of outpatient closed-loop control: First randomized crossover trials of a wearable artificial pancreas," *Diabetes Care*, vol. 37, no. 7, pp. 1789–1796, 2014.
[29] E. Renard, A. Farret, J. Kropff, D. Bruttomesso, M. Messori, J. Place, R. Visentin, R. Calore, C. Toffanin, F. D. Palma, G. Lanzola, P. Magni, F. Boscari, S. Galasso, A. Avogaro, P. Keith-Hynes, B. Kovatchev, S. Del Favero, C. Cobelli, L. Magni, and AP@home Consortium, "Day and night closed-loop glucose control in patients with type 1 diabetes under free-living conditions: Results of a single-arm 1-month experience compared with a previously reported feasibility study of evening and night at home," *Diabetes Care*, vol. 39, no. 7, pp. 1151–1160, 2016.
[30] P. Palumbo, G. Pizzichelli, S. Panunzi, P. Pepe, and A. De Gaetano, "Model-based control of plasma glycemia: Tests on populations of virtual patients," *Math Biosci.*, vol. 257, pp. 2–10, 2014. doi: 10.1016/j.mbs.2014.09.003.
[31] R. Hovorka, V. Canonico, L. J. Chassin, U. Haueter, M. Massi-Benedetti, M. Orsini Federici, T. R. Pieber, H. C. Schaller, L. Schaupp, T. Vering, and M. E. Wilinska, "Nonlinear model predictive control of glucose concentration in subjects with type 1 diabetes," *Physiol. Meas.*, vol. 25, no. 4, pp. 905–920, 2004.
[32] C. Dalla Man, R. A. Rizza, and C. Cobelli, "Meal simulation model of the glucose-insulin system," *IEEE Trans. Biomed. Eng.*, vol. 54, no. 10, pp. 1740–1749, 2007.
[33] C. Dalla Man, D. M. Raimondo, R. A. Rizza, and C. Cobelli, "Gim, simulation software of meal glucose-insulin model," *J. Diabetes Sci. Technol.*, vol. 1, no. 3, pp. 323–330, 2007.
[34] B. P. Kovatchev, M. D. Breton, C. Dalla Man, and C. Cobelli, "In silico preclinical trials: A proof of concept in closed-loop control of type 1 diabetes," *J. Diabetes Sci. Technol.*, vol. 3, no. 1, pp. 44–55, 2009.
[35] C. Dalla Man, F. Micheletto, D. Lv, M. Breton, B. Kovatchev, and C. Cobelli, "The UVA/Padova type 1 diabetes simulator: New features," *J. Diabetes Sci. Technol.*, vol. 8, no. 1, pp. 26–34, 2014.
[36] R. Visentin, C. Dalla Man, B. Kovatchev, and C. Cobelli, "The University of Virginia/padova type 1 diabetes simulator matches the glucose traces of a clinical trial," *Diabetes Technol. Therapeut.*, vol. 16, no. 7, pp. 428–434, 2014.
[37] R. Visentin, C. Dalla Man, Y. C. Kudva, A. Basu, and C. Cobelli, "Circadian variability of insulin sensitivity: Physiological input for in silico artificial pancreas," *Diabetes Technol. Therapeut.*, vol. 17, no. 1, pp. 1–7, 2015.
[38] R. Visentin, C. Dalla Man, and C. Cobelli, "One-day Bayesian cloning of type 1 diabetes subjects: Towards a single-day UVA/Padova type 1 diabetes simulator," *IEEE Trans. Biomed. Eng.*, vol. 63, no. 11, pp. 2416–2424, 2016.
[39] S. Del Favero, F. Boscari, M. Messori, I. Rabbone, R. Bonfanti, A. Sabbion, D. Iafusco, R. Schiaffini, R. Visentin, R. Calore, Y. Leal Moncada, S. Galasso, A. Galderisi, V. Vallone, F. D. Palma, E. Losiouk, G. Lanzola, D. Tinti, A. Rigamonti, M. Marigliano, A. Zanfardino, N. Rapini, A. Avogaro, D. Chernavvsky, L. Magni, C. Cobelli, and D. Bruttomesso, "Randomized summer camp cross-over trial in 5–9 year old children: Outpatient wearable artificial pancreas is feasible and safe," *Diabetes Care*, vol. 39, no. 7, pp. 1180–1185, 2016.
[40] M. Messori, M. Ellis, C. Cobelli, P. D. Christofides, and L. Magni, "Improved postprandial glucose control with a customized model predictive controller," in *Proc. American Control Conf.*, Chicago, IL, July 1–3, 2015, pp. 5108–5115.
[41] M. Messori, C. Toffanin, S. Del Favero, G. De Nicolao, C. Cobelli, and L. Magni. (2016). Model individualization for artificial pancreas. *Comput. Meth. Prog. Bio.* [Online]. Available: http://dx.doi.org/10.1016/j.cmpb.2016.06.006.
[42] G. Pillonetto and G. De Nicolao, "A new kernel-based approach for linear system identification," *Automatica*, vol. 46, no. 1, pp. 81–93, 2010.
[43] S. Del Favero, A. Facchinetti, G. Sparacino, and C. Cobelli, "Improving accuracy and precision of glucose sensor profiles: Retrospective fitting by constrained deconvolution," *IEEE Trans. Biomed. Eng.*, vol. 61, no. 4, pp. 1044–1053, 2014.
[44] M. Messori, C. Toffanin, S. D. Favero, G. D. Nicolao, C. Cobelli, and L. Magni, "A nonparametric approach for model individualization in an artificial pancreas," *IFAC-Papers OnLine*, vol. 48, no. 20, pp. 225–230, 2015.
[45] C. Ellingsen, E. Dassau, H. Zisser, B. Grosman, M. W. Percival, L. Jovanovic, and F. J. Doyle, III, "Safety constraints in an artificial pancreatic beta cell: An implementation of model predictive control with insulin on board," *J. Diabetes Sci. Technol.*, vol. 3, no. 3, pp. 536–544, 2009.
[46] L. Magni, D. M. Raimondo, C. Dalla Man, M. Breton, S. Patek, G. De Nicolao, C. Cobelli, and B. P. Kovatchev, "Evaluating the efficacy of closed-loop glucose regulation via control-variability grid analysis," *J. Diabetes Sci. Technol.*, vol. 2, no. 4, pp. 630–635, 2008.
[47] D. M. Maahs, B. A. Buckingham, J. R. Castle, A. Cinar, E. R. Damiano, E. Dassau, J. H. DeVries, F. J. Doyle, III, S. C. Griffen, A. Haidar, L. Heinemann, R. Hovorka, T. W. Jones, C. Kollman, B. Kovatchev, B. L. Levy, R. Nimri, D. N. O'Neal, M. Philip, E. Renard, S. J. Russell, S. A. Weinzimer, H. Zisser, and J. W. Lum, "Outcome measures for artificial pancreas clinical trials: A consensus report," *Diabetes Care*, vol. 39, no. 7, pp. 1175–1179, 2016.